# Whole-brain Background Functional Connectivity Patterns Capture Differences Between Perception and Retrieval States

Y. Peeta Li[1*], Yida Wang[2], Nicholas B. Turk-Browne[3,4], Brice A. Kuhl[1], J. Benjamin Hutchinson[1]

[1] Department of Psychology, University of Oregon, Eugene, OR

[2] Amazon Web Services, Palo Alto, CA

[3] Department of Psychology, Yale University, New Haven, CT

[4] Wu Tsai Inst., Yale Univ., New Haven, CT

∗ Corresponding Author.
*E-mail address*: peetal@uoregon.edu (Y.Peeta Li).

**ABSTRACT**

Externally- and internally-oriented cognitive states of perception and retrieval determine whether the same visual input becomes the target of visual perception or the trigger for episodic memory retrieval. Previous research suggested that differences between the two cognitive states are reflected in intrinsic function connectivity (FC) patterns across large-scale cortical networks. Here, leveraging recently developed methods for quantifying intrinsic "background" connectivity using full correlation matrix analysis (FCMA), we conducted an unbiased whole-brain analysis to compare intrinsic FC configurations underlying perception and retrieval states. This investigation revealed 16 clusters across 3 functional network communities whose intrinsic FC patterns best characterized and discriminated the two cognitive states. In particular, clusters in the control-related network showed increased connectivity during the perception state, whereas clusters in the default mode network (DMN) were more strongly coupled during the retrieval state. Importantly, we found that the retrosplenial cortex (RSC) switched its connectivity patterns from coupling with the control network to the DMN as the cognitive state shifted from retrieval to perception. Additional pattern analyses suggest that RSC plays a crucial role in establishing perception and retrieval states, which is in line with the theory that RSC bridges exogenous and endogenous information processing. Together, our results provide a comprehensive but interpretable view of the neural markers that characterize and differentiate between perception and retrieval states.

**INTRODUCTION**

Visual perception constructs external representations of the current world while episodic memory retrieval assembles internal representations of the past (Carrasco et al., 2004; Tulving, 2002). Throughout our daily life, we track the surrounding environment while maintaining a stream of internal thoughts. Interestingly, however, the same visual input can potentially be both the target of perception and the trigger for episodic retrieval. In this respect, the brain must steadily sustain within and appropriately switch between the states of perception and retrieval, such that the perceptual or/and mnemonic information related to the ongoing input can be obtained efficiently when needed. Previous research has suggested that perception and retrieval states often engage similar neural substrates, but the functional interaction patterns among constituents of these networks may differ across states (Cooper & Ritchey, 2019; Duncan et al., 2014; Lee et al., 2019; Linde-Domingo et al., 2019; O'Reilly & McClelland, 1994; Schacter et al., 1998). Yet these investigations primarily focused on a limited set brain regions defined a priori (e.g., medial temporal lobe) and thus may overlook important changes in network configuration throughout the brain. As both perception and retrieval states may rely on coordinated activity distributed across the brain, a more comprehensive analysis comparing the whole-brain functional interaction patterns during the two cognitive states may reveal novel neural substrates for switching and sustaining states (Turk-Browne, 2013; Wang et al., 2015). As such, the goal of the current work is to investigate and identify the neural markers that characterize and differentiate between perception and retrieval states from a whole-brain perspective.

The distinctions between perception and retrieval are usually studied by comparing stimulus-driven activation patterns during perceiving and retrieving the same episode; for example, by comparing representational content under the two tasks (Bosch et al., 2014; Kuhl & Chun, 2014; H. Lee & Kuhl, 2016; Xiao et al., 2017) or the spatial extent or displacement in neural representation (Favila et al., 2020; Long & Kuhl, 2021). These works primarily focused on interpreting stimulus-driven brain activity and do not adequately address state-related neural processes: the intrinsic functional network architecture of the brain essential for maintaining sustained perception or retrieval states (Summerfield et al., 2006; Turk-Browne et al., 2010). As such, the challenge for identifying neural markers for perception and retrieval states is to distinguish the "state-related" neural processes from those that are "stimulus-related". To overcome such problems, the current work uses "background" functional connectivity (FC) analysis to isolate "state-related" neural processes (Al-Aidroos et al., 2012; Córdova et al., 2016; Norman-Haignere et al., 2012). Background FC refers to the temporal correlations between brain regions after modeling and removing the stimulus-evoked response from each regions (Cole et al., 2019; Norman-Haignere et al., 2012). Previous research suggests that patterns of background FC reliably reflect ongoing cognitive process by strengthening functional pathways that are important for achieving certain cognitive goals (Al-Aidroos et al., 2012; Duncan et al., 2014; Turk-Browne, 2013). In this respect, comparing background FC

patterns supporting the perception and retrieval states could reveal important neural dynamics for maintaining a sustained state or differentiating between the two states.

To date, only a few works have compared perception vs. retrieval states by examining background connectivity patterns but have narrowed the scope of their network analyses to a specific brain region or functional community (Cooper & Ritchey, 2019; Duncan et al., 2014) . For example, one recent study examined background FC patterns exclusively between memory-related brain regions in the parietal-memory (PM) and anterior-temporal (AT) networks during perception versus retrieval (Cooper & Ritchey, 2019). Specifically, they showed that regions in these networks exhibited stronger background connectivity during retrieval compared to perception state, thus providing a neural marker for maintaining a sustained retrieval state. Despite the utility of these targeted, seed-based analyses, the previous research may lose sight of both finer-grained network configurations and important interactions beyond memory-related networks (Beckmann et al., 2005; Turk-Browne, 2013). Perception and retrieval are complex cognitive states that may involve interaction changes across the whole brain (Geib et al., 2017; Shinkareva et al., 2008; Vuilleumier & Pourtois, 2007). For example, many prior studies have provided evidence that the frontoparietal control network and other attention-related networks are also related to recollection along with the conventional memory-related regions (Fornito et al., 2012; Robin et al., 2015; Schedlbauer et al., 2014; St Jacques et al., 2011; Westphal et al., 2017). Thus, the investigation of perception versus retrieval states would benefit from whole-brain background FC pattern analysis. It is important to note that conducting whole-brain voxel-level FC analyses is often computationally intractable (a whole-brain analysis of 50k voxels will yield a 1.25B-long connectivity vector), and although the benefits of such analyses has long been established, previous attempts usually compromised the number of brain regions included in the analyses (e.g., Pantazatos et al., 2012; Watanabe et al., 2012). Here we applied the recently-developed full correlation matrix analysis (FCMA) to perform whole-brain, voxel-level background FC analysis (Kumar et al., 2022; Turk-Browne, 2013; Wang et al., 2015). FCMA relies on high-performance kernel-based analysis and parallel computing to reduce computation time from days to hours and has been shown to reveal important connectivity changes beyond those identified using conventional seed-based analysis (Wang et al., 2015)

The current study aims to identify intrinsic functional connectivity (FC) dynamics that characterize and differentiate between perception and retrieval states by examining and comparing the whole-brain background FC patterns during the two states. To do this, we designed an experiment in which participants performed either a perception or retrieval task on the same series of images. Importantly, the tasks were matched in terms of both visual content and task accuracies such that the identified background FC components are specific to differences in maintaining a sustained cognitive state (i.e., perception vs. retrieval) instead of potential differences in other aspects (i.e., visual categories and task

difficulty). We applied FCMA in combination with permutation-based statistical inference to identify important differences in background FC between perception and retrieval states; we then used connectivity density and pattern similarity analyses to interpret such differences and the role of brain regions involved. In brief, the current work revealed four important findings: (1) maintaining sustained cognitive states of perception and retrieval engage distinct whole-brain background FC architectures; (2) perception and retrieval states could be discriminated based on background FC patterns between 16 clusters that are grouped into three functional communities—the control network, default mode network (DMN), and retrosplenial cortices (RSC); (3) the control and default mode networks demonstrated stronger intra-network connectivity densities during perception and retrieval states, respectively; and (4) the RSC coupling pattern with the control and default mode networks shifted as a function of cognitive state, suggesting that it could potentially be an important hub for transitioning between perception and retrieval.

## RESULTS

### Perception and Retrieval Tasks

We designed tasks that required participants to attend to information that was either sensory (perception) or mnemonic (retrieval), with the experimental conditions otherwise matched in terms of visual content and task difficulty (**Figure 1a**). Specifically, during a behavioral training session, 24 participants were extensively trained to remember pairs of face-scene associations, with the faces being either male or female and the scenes being either man-made or natural scenes. For each block (epoch) in the scanner, participants were presented with a series of either faces or scenes. During the *Perceive* condition, participants were asked to make either a male/female or man-made/natural decision for the visually-presented image. In contrast, during the *Retrieve* condition, participants were instructed to retrieve the image that was associated with the visually-presented image and to make a male/female or man-made/natural decision for that retrieved image. Note that perception and retrieval tend to differ in cognitive demands, with the latter being more demanding. To account for the potential difference introduced by task difficulties, we introduced a third condition, the *Scramble* condition. Specifically, participants performed the same perception task as in the *Perceive* condition, but with visually scrambled cue presentations to increase the task difficulty of a perception task. The level of the blurriness was titrated through behavioral piloting to match the performance accuracies between the *Retrieve* and *Scramble* conditions. Participants performed 16 epochs of each task condition, evenly divided into 2 fMRI runs, resulting in a total of 6 fMRI runs, and the order of the task conditions was randomized across participants. **Figure 1b** shows the behavioral task performance for each task condition. One-way (condition) repeated measure ANOVAs revealed a main effect of condition for both reaction time ($F_{(2, 46)}$ = 288.8, $p < 0.001$, $\eta^2 = 0.97$) and performance accuracy ($F_{(2, 46)} = 91.21$, $p < 0.001$, $\eta^2 = 0.90$). Importantly,

although performance accuracy of the *Perceive* condition is significantly greater than that of *Retrieve* condition ($t_{(23)} = 13.4$, $p < 0.001$, 95% CI = [0.16, 0.22], Cohen's d = 3.55), it was successfully matched between *Retrieve* and *Scramble* conditions such that they did not differ in task performance ($t_{(23)} = -1.65$, $p = 0.11$, 95% CI = [-0.07, 0.01], Cohen's d = 0.45).

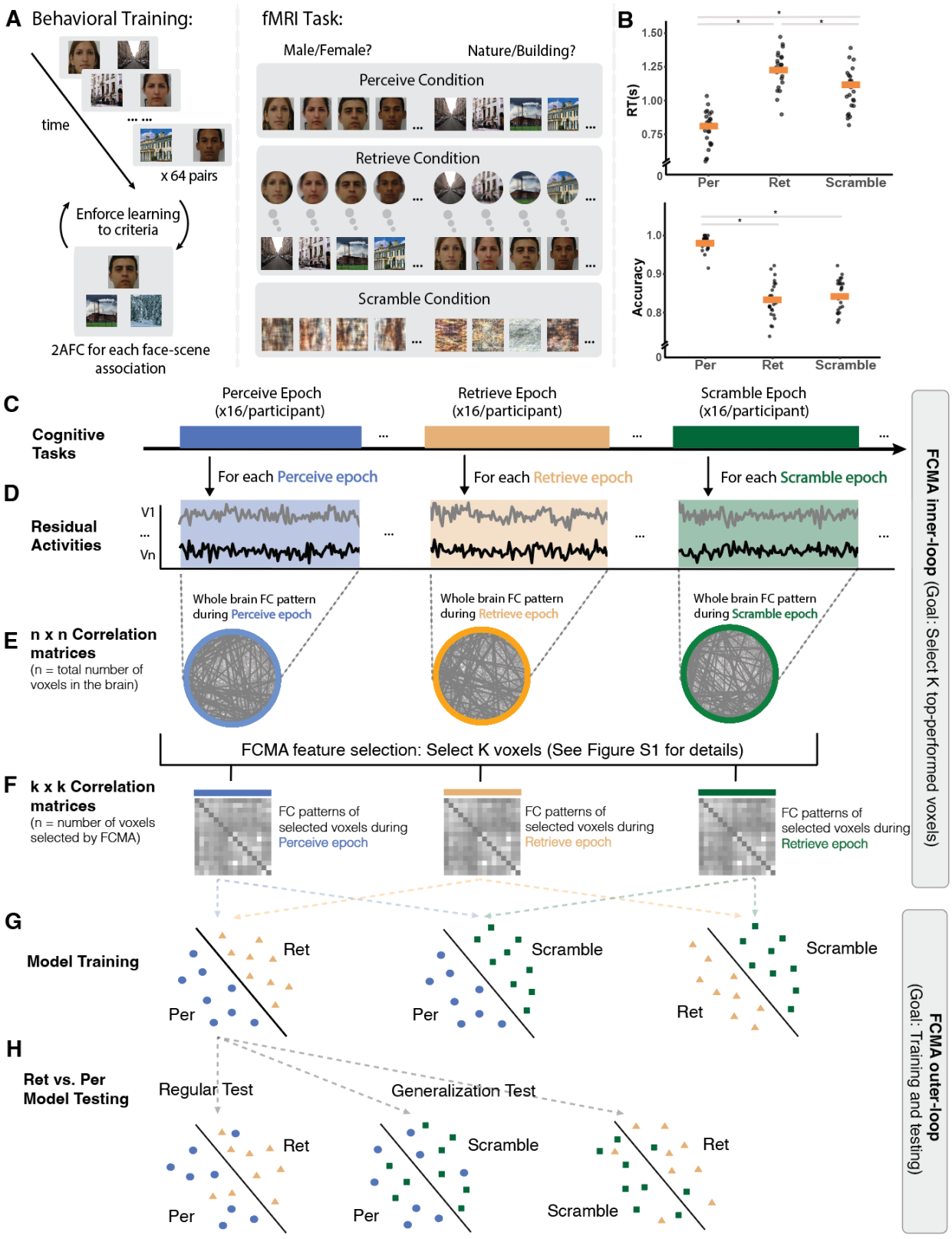


**Figure 1.** Task paradigm and analysis flowchart. **A**) The task paradigm for behavioral training and in-scanner task designs. **B**) In-scanner behavioral performance, with the orange bar indicating the sample

mean and asterisks indicating $p < 0.05$ **C**) Each condition had 16 epochs for each participant, with each epoch lasting 40 seconds long. **D**) The residual activity for each task epoch was computed by regressing out the stimulus-evoked component using a finite impulse response general linear model. **E**) Whole-brain voxel-wise background FC matrices were computed for each task epoch. These matrices are shaped *n* by *n*, where *n* is the total number of voxels in the brain ($n = 92745$). **F**) Background FC matrices of FCMA-selected voxels. FCMA was implemented to select a certain number of voxels whose connectivity patterns were highly accurate for separating perception and retrieval states. The details of the feature selection process are shown in **Figure S1**. In this way, FCMA reduced the whole-brain correlation matrix to a *k* by *k* correlation matrix for each epoch, where *k* is the number of voxels selected by FCMA. The current study tested multiple values of *k*, ranging from 100 to 15000. **G**) Model training. Using a cross-validation framework, SVM classifiers with precomputed linear kernel were trained to separate all task condition comparisons. **H**) Model testing. The trained models were tested using the left-out subject for each fold. During the regular test, the model was tested on the same task condition comparison as the one it was trained on. During the generalization test, the model was tested on a different task condition comparison from the one it was trained on.

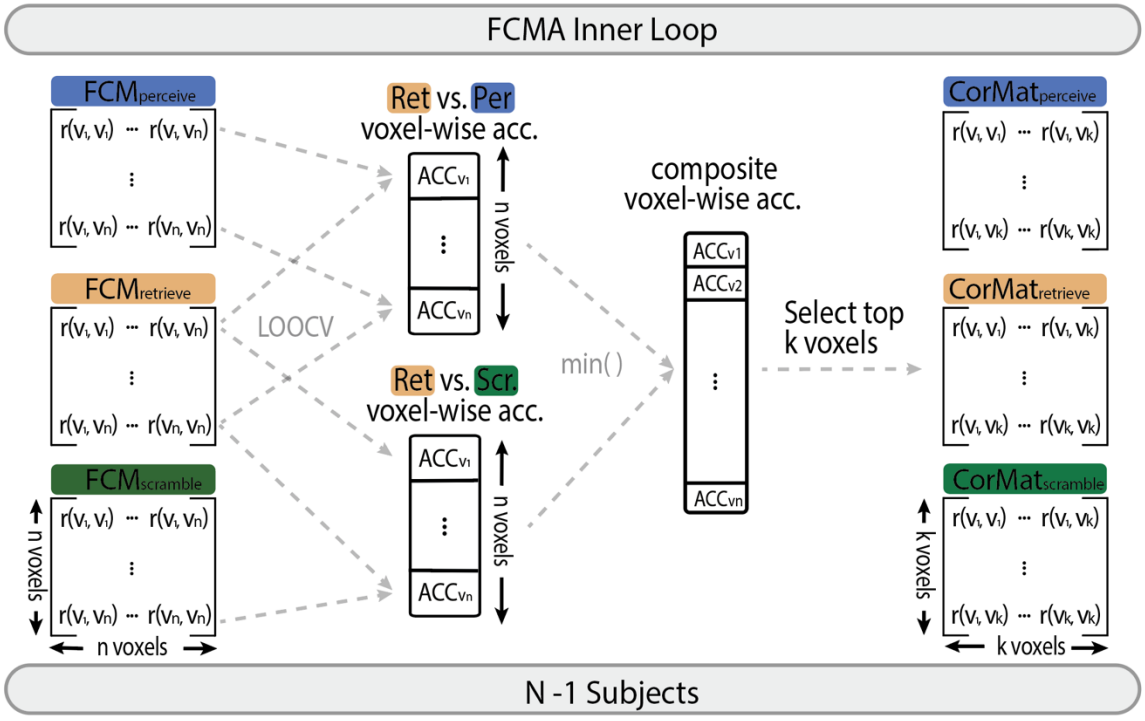


**Supplementary Figure 1.** FCMA feature selection paradigm. Within each training fold, we examined the degree to which each voxel's background functional connectivity patterns (seed map) can be used to differentiate Retrieve vs. Perceive comparison and Retrieve vs. Scramble comparison. This leads to two n-vector accuracy measures, one for each task condition comparison. A composite voxel-wise accuracy score was computed by taking the minimum accuracy value for each voxel across the two n-vectors. The top k number of voxels in terms of their composite accuracy scores were selected to construct the dimension reduced FC patterns (**Figure 1F**). Note that a different (but typically highly-overlapping) set of *k* voxels would be selected for each training fold. As a result, the full cross-validation framework would create 24 masks (nonidentical but highly overlapping) for each choice of *k*.

**Perception and Retrieval Involve Distinct Intrinsic Connectivity Patterns**

We first examined whether perception and retrieval states indeed involve systematically different "state-related" whole-brain FC patterns. Using background connectivity analysis, the stimulus-evoked component of the preprocessed blood oxygen level dependent (BOLD) time series was regressed out using a general linear model (Cole et al., 2019). The residuals were then used for computing voxel-wise whole-brain temporal correlation matrix for each epoch, yielding 16 subject-specific whole-brain background FC matrices for each of the three conditions (each FC matrix is shaped 92745 voxels by 92745 voxels; **Figure 1e**). To examine the potential differences between background FC patterns associated with perception and retrieval states, we applied full correlation matrix analysis (FCMA) to test whether a trained SVM could successfully separate perception epochs (i.e., *Perceive* and *Scramble*) from

retrieval epochs (i.e., *Retrieve*). FCMA was designed to perform classification analyses on voxel-wise whole-brain FC patterns in a computationally efficient way. Through a nested leave-one-subject-out cross-validation framework, FCMA selected voxels whose correlation patterns (seed map) best differentiate between perception versus retrieval states, thus reducing the FC pattern size to a tractable size (**Figure 1f**; **Figure S1**; See **Methods: *Full Correlation Matrix Analysis on Residual Activity***). SVMs with precomputed linear kernel were then trained based on the FC patterns of tractable sizes to classify the task conditions (**Figure 1g, h**).

FCMA selected an arbitrary size of *k* best performed voxels to construct the tractable FC patterns. We started by selecting a small set of voxels ($k = 100$) and gradually increased the size until improvements in classifier performance reached an asymptote. Here we reported results for the 3000 voxel masks as we found that the model performances nearly plateaued at around this size for separating state-related differences (i.e., perception vs. retrieval), but the pattern of the results were qualitatively similar when other sizes of the masks were used. To evaluate binary classifier performances, we computed the receiver operating characteristic (ROC) curves and the area under the ROC curve (AUC) for each classifier per subject, with larger AUC indicating better model performance (Hanley & McNeil, 1982).The results suggest that classifiers trained on background FC patterns of the FCMA-selected set of voxels successfully differentiated epochs of perception from retrieval states (*Perceive* vs. *Retrieve*: $M_{auc} = 0.87 \pm 0.06$, $t_{(23)} = 28.62$, $p < .001$, 95% CI = [0.84, 0.89], Cohen's d = 5.84; *Retrieve* vs. *Scramble*: $M_{auc} = 0.83 \pm 0.08$; $t_{(23)}$ 19.39, $p < .001$, 95% CI = [0.79, 0.86], Cohen's d = 3.96; one-sample t-test with $\bar{\mu} = 0.5$ which indicates chance level performance; **Figure 2a**; see **Figure S2a** for results on percentage accuracy). Notably, additional analyses suggested that state-related differences were selectively captured by background FC measures, instead of any left-over stimuli-evoked components in the residual timeseries. In particular, models trained using residual activity patterns (i.e., simple MVPA on residual timeseries) of the same voxel masks failed to discriminate any task condition comparisons (all model performances ≈ 50%; **Figure S2b**). One potential counter argument is that the above-chance performance of these background FC classifiers was not strictly related to differences in perception versus retrieval states. In this respect, *Perceive* vs. *Retrieve* comparison can be separated based on task difficulties whereas *Scramble vs. Retrieve* comparison is differentiable based on visual contents (i.e., scrambled vs. intact stimuli). To demonstrate that the variations in background FC patterns (among FCMA-selected voxels) were most strongly induced by state-related differences, we performed two extra sets of analyses to rule out the potential confounds discussed above. First, we tested the background FC pattern separability of *Perceive* vs. *Scramble* conditions—a task condition comparison that differed in terms of both task difficulty and visual contents *but not* in cognitive state. Thus, if the background FC patterns contains mostly state-related information, the lack of state-related differences in the *Perceive* vs. *Scramble* comparison should lead to worse performance of the classifier. As expected, a one-way ANOVA shows

that the AUC significantly differed between the non-state-related and state-related (background) FC classifiers ($F_{(2,69)}$ = 14.72, $p < 0.001$, $\eta^2$ = 0.30), with that of the *Perceive-Scramble* FC classifier being significantly smaller than other FC classifiers (compared with *Retrieve-Perceive*: $t_{(46)}$ = -5.04, $p < 0.001$, 95% CI = [-0.19, -0.08], Cohen's d = 1.45; Compared with *Retrieve-Scramble*: $t_{(46)}$ = -3.37, $p < 0.001$, 95% CI = [-0.16, -0.04], Cohen's d = 0.97; **Figure 2b left**). No significant difference was observed between the other two FC classifiers ($t_{(46)}$ = 1.82, $p$ = 0.08, 95% CI = [-0.01, 0.08], Cohen's d = 0.52).

In the second set of analyses, we aimed to further quantify the degree to which the background FC classifiers are sensitive to differences from each of the three dimensions: (1) cognitive state (i.e., perception vs. retrieval); (2) task difficulty; and (3) visual content. Sensitivities were quantified as how well a trained background FC classifier could be generalized to differentiate a different task condition comparison (**Figure 1f**), with the assumption being that generalizability should be the greatest for task condition comparisons that both involved state-related differences (i.e., *Perceive* vs. *Retrieve* and *Scramble* vs. *Retrieve***; Figure S3b**). Consistent with what we previously observed, our results suggest that background FC classifiers showed distinct sensitivity to the three dimensions (sensitivities were quantified as bidirectionally averaged generalization AUC: cognitive task state: $M_{\text{auc}}$ = 0.78 $\pm$ 0.07; task difficulty: $M_{\text{auc}}$ = 0.68 $\pm$ 0.07; visual content: $M_{\text{auc}}$ = 0.53 $\pm$ 0.11; $F_{(2,69)}$ = 52.80, $p < 0.001$, $\eta^2$ = 0.60, **Figure S3a**) and are significantly more sensitive to state-related differences compared to other dimensions (all $p < 0.001$). Together, these results suggest that background FC patterns (among FCMA-selected voxels) selectively capture state-related differences between perception and retrieval states, and were minimally driven by differences in other dimensions.

**Background Connectivity and Evoked Activity Patterns Capture Distinct Aspects of Cognitive Processes**

Previous research has provided compelling evidence that stimulus-evoked multi-voxel activation patterns could reflect ongoing cognitive processes and can be used to train classifiers for separating task condition comparisons (Long & Kuhl, 2021; Norman et al., 2006). Nevertheless, it is unclear whether background functional connectivity (FC) and evoked activity patterns reflect similar or distinct aspects of the cognitive processes. Here, we sought to further examine the potential differences between these two neural measures. Specifically, we used stimulus-evoked activation patterns to train MVPA classifiers for separating each task condition comparison and then compared their performances to those trained using background FC patterns (**Figure 2b left and middle**). As expected, (stimulus-evoked) MVPA classifiers also succeeded in separating the task conditions (all $p < 0.001$; One-sample t-test with $\bar{\mu}$ = 0.5). Interestingly, however, we did not observe the preference for state-related differences in MVPA classifiers. That is, when comparing MVPA classifiers using AUC, *Retrieve* vs. *Perceive* and *Scramble* vs. *Perceive* classifiers demonstrated comparable performance, even though only the former comparison

involved state-related distinction (*Retrieve* vs. *Perceive*: $M_{auc}$ = 0.86 ± 0.06, *Scramble* vs. *Perceive*: $M_{auc}$= 0.90 ± 0.12; $t_{(46)}$ = 0.42, $p$ = 0.67, 95% CI = [-0.05, 0.07], Cohen's d = 0.12; **Figure 2b middle**). A two-way ANOVA confirmed that there is an interaction between classifier type (e.g., *Retrieve* vs. *Perceive* classifier) and neural measure type (i.e., background FC vs. stimulus-evoked activity patterns; $F_{(2,138)}$ = 6.60, $p$ = 0.002, $\eta^2$ = 0.09), suggesting that classifier performances differed based on the type of neural measure the classifiers were trained with. In this aspect, the two neural measures may indeed capture non-overlapping components of cognitive processes. To test this hypothesis, we adopted the method used by Manning et al. (2018) and trained hybrid classifiers that assembled decision confidences from both FC and MVPA classifiers for separating condition comparisons. That is, the decision confidences of the hybrid classifier were computed as the averaged decision function outputs from both FC and MVPA classifiers. The rationale is that the hybrid classifiers should achieve better performance if the two neural measures make distinct contributions in discriminating the cognitive processes (Manning et al., 2018). As expected, a two way ANOVA revealed a significant main effect of neural measures ($F_{(2,207)}$ = 59.68, $p$ < 0.001, $\eta^2$ = 0.06; **Figure 2b**). Follow-up analyses showed that the averaged AUC of hybrid classifiers was significantly higher than those of background FC classifiers ($t_{(46)}$ = 8.95, $p$ < 0.001, 95% CI = [0.11, 0.17], Cohen's d = 2.58) and also numerically higher than evoked-activation MVPA classifiers ($t_{(46)}$ = 1.67, $p$ = 0.10, 95% CI = [-0.01, 0.06], Cohen's d = 0.88). Together, these results suggest that background FC and evoked activation patterns capture different sources of cognitive processes, with the former capturing more state-related (e.g., perception vs. retrieval states) information.

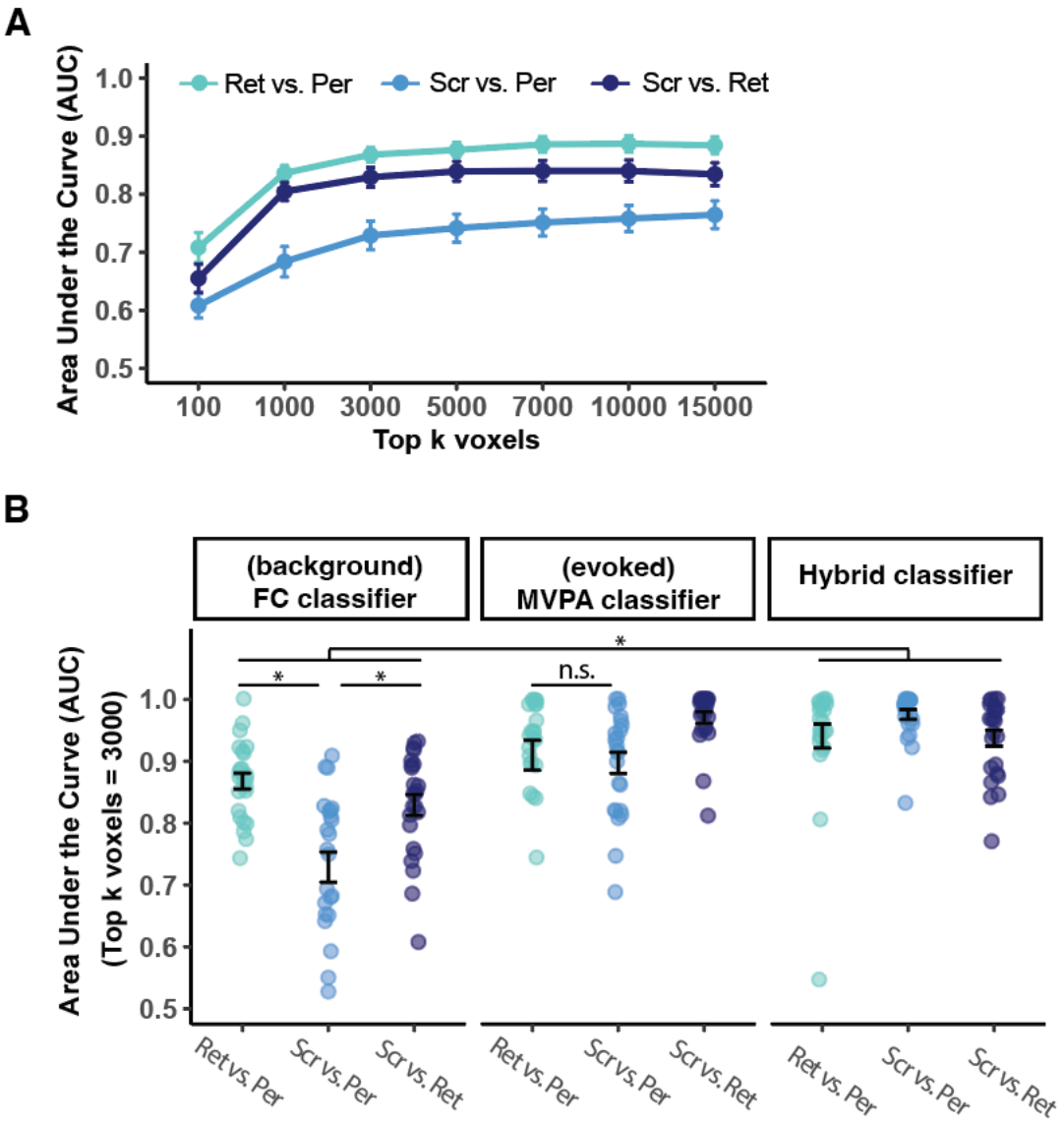


**Figure 2.** Classifier performance for differentiating task condition comparisons using different types of neural measures. **A**) Performance of background FC classifiers as a function of the number of voxels selected by the FCMA algorithm. Area under the receiver operating characteristic curve (AUC) was computed for each leave-one-subject-out testing fold to examine the performance of the binary classifiers. The error bars indicate the standard error of the mean AUC across testing folds. **B**) Comparing performance of binary classifiers trained with different neural measures. The hybrid classifier's decision function outputs were computed as the average of the decision function outputs from FC and MVPA classifiers.

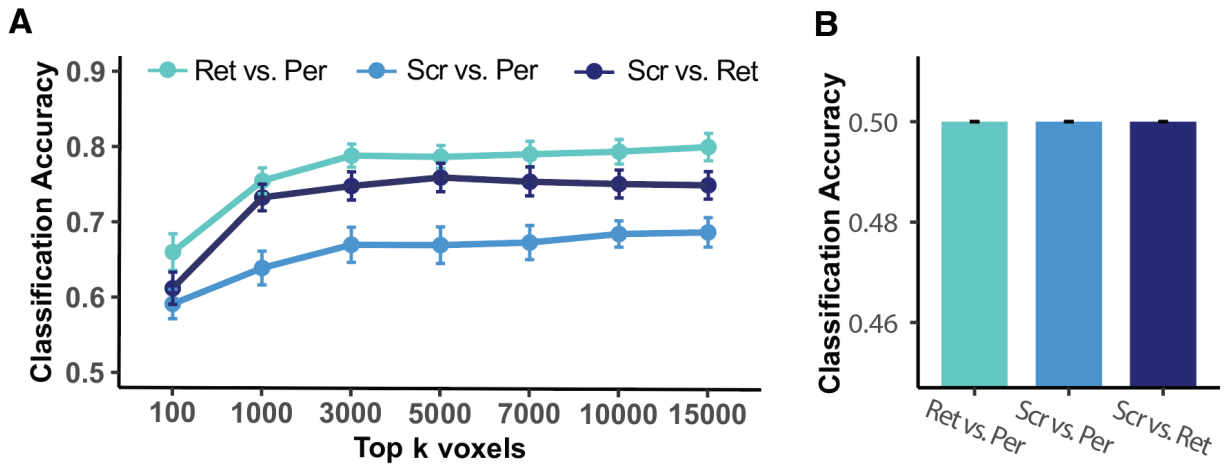


**Supplementary Figure 2.** Performances (as measured by model accuracies) of classifiers trained on background FC patterns and residual activity pattern (i.e., MVPA classifiers trained on residual activity patterns) for separating task condition comparisons. **A)** Model classification accuracies for each comparison across different size of the voxel mask. When k = 3000: *Perceive-Scramble*: $M_{acc}$ = 0.67% ± 0.11%; *Perceive-Retrieve*: $M_{acc}$ = 0.79% ± 0.08%; *Retrieve-Scramble*: $M_{acc}$ = 0.75% ± 0.09%. **B)** Using the *k* = 3000 mask, MVPA classifiers were trained on residual activity patterns for differentiating each comparison. Note that we did not compute AUC for these classifiers due to the observable chance-level performances.

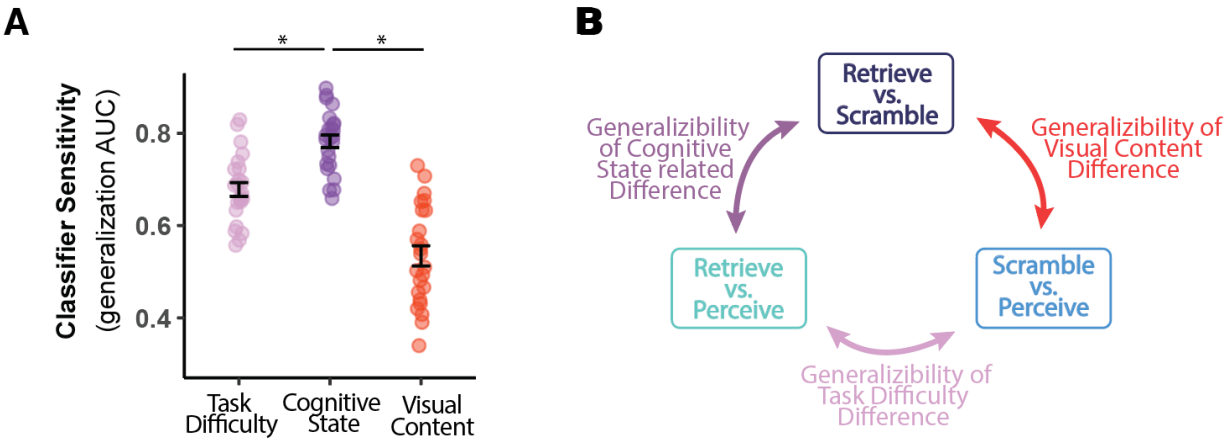


**Supplementary Figure 3. A**) Sensitivity of background FC classifiers to three distinctions that include cognitive state (i.e., perception vs. retrieval), visual content (i.e., scrambled vs. intact), and task difficulty (i.e., low vs. high accuracies). Sensitivity was quantified as the bidirectionally averaged AUC between background FC classifiers trained to differentiate each distinction (generalization test). **B**) Schematic diagram for measuring sensitivity to different aspects of cognitive processes using generalization tests. For example, given that both *Retrieve* vs. *Scramble* and *Retrieve* vs. *Perceive* comparisons involve state-related differences, the degree to which the background FC classifier trained on *Retrieve* vs. *Scramble*

comparison could be generalized to classify *Retrieve* vs. *Perceive* comparison would suggest the sensitivity of FC patterns to state-related differences.

**Perception and Retrieval States are Discriminated Based on Background FC Between 16 Brain Regions Grouped into 3 Functional Communities**

The results so far suggest that background FC patterns of FCMA-selected voxels preferentially captured differences between perception and retrieval cognitive states. Nevertheless, due to our use of a leave-one-subject-out cross validation framework, different sets of voxels were selected by FCMA for different left-out subject in the testing fold. To allow further characterization and interpretation of state-related background FC patterns, we combined the FCMA inner loop (**Figure S1**) with permutation-based statistical inference tests to obtain a shared set of voxels across all testing folds (yielding roughly 4000 voxels) whose background FC patterns capture state-related differences (for details see **Methods**: ***Information Mapping***). With this shared voxel mask, however, it may still be intractable to interpret FC patterns consisting of thousands of connections (there are $\sim 8 \times 10^6$ distinct connections among 4000 voxels). For this reason, we further reduced the dimensions of FC patterns using a clustering method. First, we identified spatially adjacent clusters of voxels in the shared mask; second, we selected clusters whose FC variations contributed to the task condition discrimination performance. That is, we trained classifiers to differentiate each task condition comparison, starting with all voxels within the largest cluster, and sequentially included voxels from the next largest cluster until the benefit of adding in clusters on discrimination performance plateaued (**Figure S4a**). This FCMA-then-clustering pipeline revealed to 16 clusters of interests, whose cluster-level background FC patterns should best reflect the distinction between perception and retrieval states (**Figure 3a**; **Table 1**). This pipeline is advantageous in that, in addition to its great interpretability, FC patterns between these clusters also retained superior model performances inherited from the fine-grained voxel-level FC analysis (Feilong et al., 2021; Wang et al., 2015). Quantitively, by repeating the analysis pipeline with predefined brain parcels (instead of fine-grained voxel-wise analysis), we showed that the 16 clusters derived from voxel-level analyses had significantly greater discrimination performance compared to the best performing 16 predefined parcels in the parcel-level analysis ($F_{(1,138)} = 60.25$, $p < 0.001$, $\eta^2 = 0.30$; **Figure S4b right**). Note that this result held across different parcellation granularities (400 and 1000 parcels; Schaefer et al., 2018). Moreover, follow-up analyses demonstrated that the cluster-level background FC patterns retained its preference for revealing state-related over non-state-related differences was after dimension reduction (**Figure S4a**, **b**; $F_{(2,69)} = 19.31$, $p < 0.001$, $\eta^2 = 0.36$; *Scramble* vs. *Perceive* classifier had the worst model performance; all $p < 0.001$).

Previous research suggested that functionally coupled brain regions form large scale functional communities (Yeo et al., 2011), and that a cluster may be associated with different functional community

across different cognitive states (Braun et al., 2015). With this in mind, we next examined the functional community structures of the 16 clusters of interest during each task condition (i.e., *Perceive*, *Retrieve*, and *Scramble*). Specifically, we applied the Louvain community detection algorithm (Blondel et al., 2008) to the group-averaged background FC matrices for each condition. The algorithm was repeated 1000 times on each weighted graph and the partition that maximized the modularity measure for each condition was selected (Rubinov & Sporns, 2011). Interestingly, our results suggested that the community structures underlying all three task conditions were consistent such that the 16 clusters were consistently partitioned into 3 functional communities (**Figure 3b**). The first functional community consisted of regions from the conventional default mode network (DMN; Buckner et al., 2008), including the bilateral inferior parietal lobule, precuneus, medial prefrontal cortex, posterior cingulate cortex, and the middle temporal gyrus, which hereafter we refer to as the DMN network. The second functional community consisted of the bilateral prefrontal cortex, bilateral intraparietal sulcus, superior frontal gyrus, and temporal gyrus, most of which are part of the frontoparietal network (Marek & Dosenbach, 2018); we refer to this as the Control network. The last community consists of ventral and dorsal retrosplenial cortices (RSC; Gilmore et al., 2016). We further examined the activation profiles of clusters within these 3 functional communities during each task conditon, using the beta values estimated by the FIR model (**Figure S5**; see **Method: *Stimulus-Evoked and Residual Activity***). We found that DMN clusters are task-negative during both perception and retrieval states whereas Control network clusters are task-positive across the two states. These task-negative and task-positive regions are comparable to those observed in previous works (Kim et al., 2015). Interestingly, the activation profile of RSC clusters differed between perception and retrieval states, with its being task-positive during retrieval state but task-negative during perception state. Importantly, the force-directed plots in **Figure 3b** suggested that RSC was more closely connected with the Control network during retrieval (i.e., *Retrieve* condition) but coupled more strongly with the DMN network during perception (i.e., *Perceive* and *Scramble* conditions). We examined this observation in a more quantifiable manner in the next section.

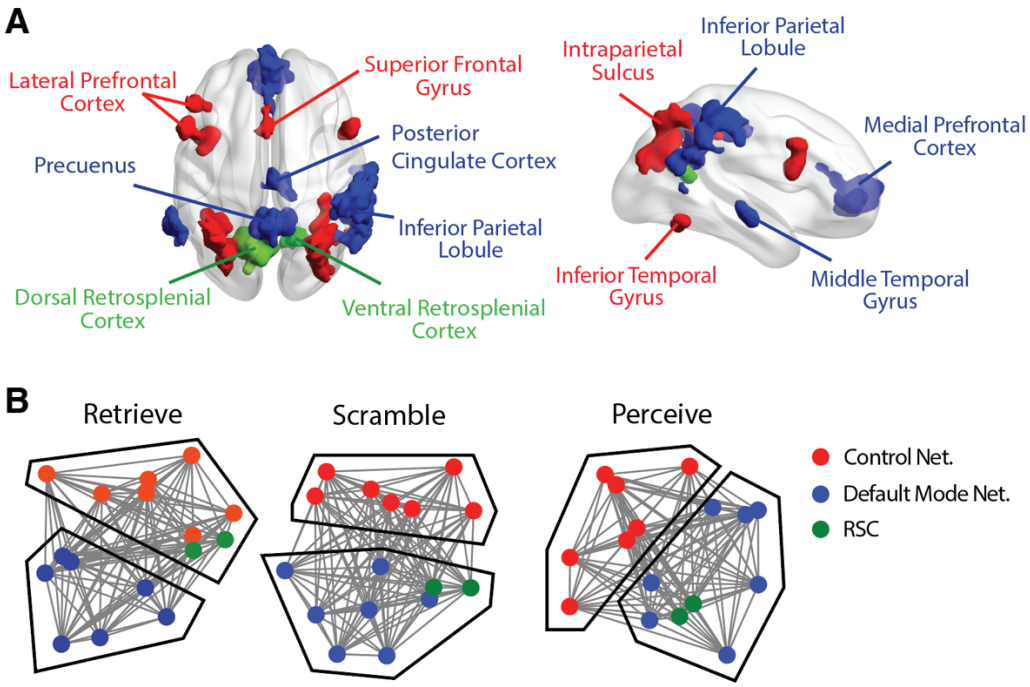


**Figure 3**. Clusters of interest and functional community structures. **A**) The 16 clusters of interest identified through the information mapping pipeline, which were further partitioned into 3 functional communities. The color indicates the functional community assignment of each cluster. **B**) The force-directed graphs were generated using the Fruchterman-Reingold force-directed algorithm implemented in NetworkX (V2.7.1; Fruchterman & Reingold, 1991). The projected physical distance in the graph indicates the functional relevance of the clusters. The color indicates the functional community allegiance of each cluster.

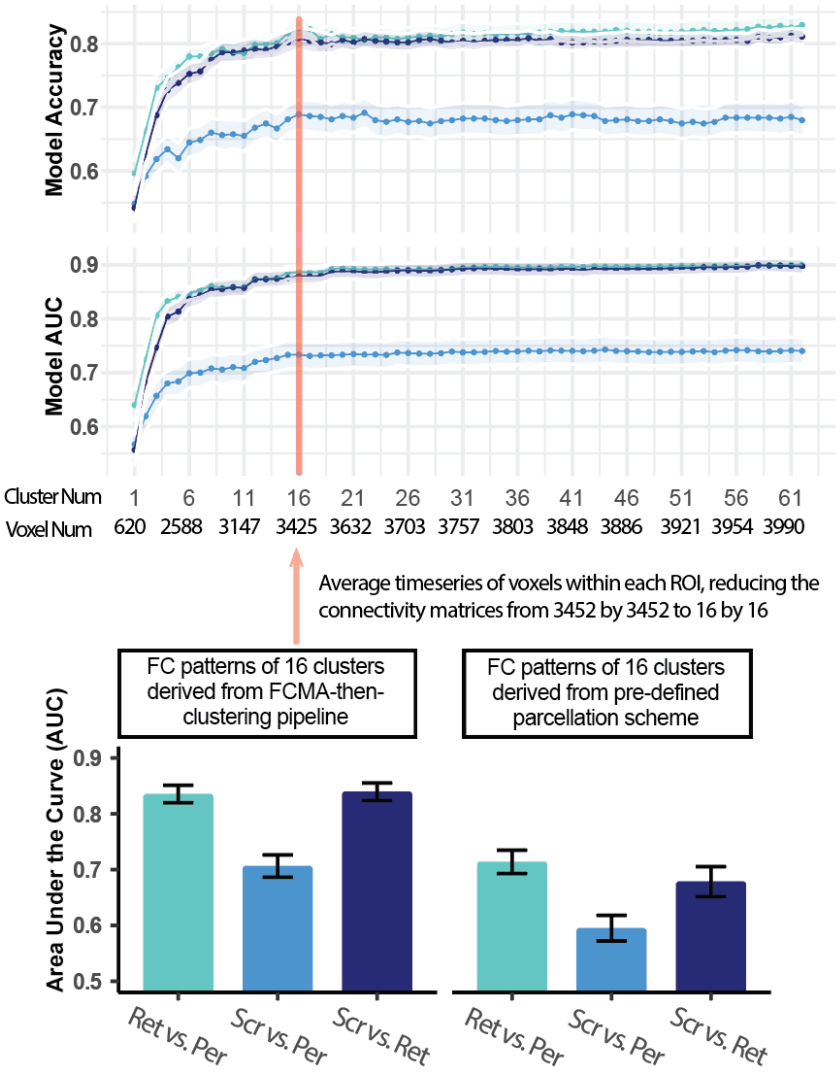


**Supplementary Figure 4** Cluster selection diagram**. A)** Model performance as measured by both percentage accuracy and area under the curve (AUC) when sequentially adding in all voxels from the next largest cluster. For example, we started by using the background FC matrices of all voxels only in the largest cluster (i.e., shaped 620 x 620) to differentiate each task condition comparison. Then we added in all voxels (nVoxel = 519; **Table 1**) form the next largest clusters and estimated the model performances of the enriched background FC matrices (now shaped 1139 x 1139), and so force. When selecting the number of clusters to be included in subsequent analyses, we used accuracy as optimizing metric because the models need to successfully differentiate task condition comparisons; and we used AUC as satisficing metric to meet the expectation of the discrimination capacity. We noticed that when including all voxels from the top 16 clusters, the model reached its peak accuracy while maintaining a descent AUC. **B**) **Left**: We averaged all voxels within a cluster, thus reducing the dimensions of the FC matrices from 3452 x 3452 to 16 x 16. We then examined the performances of the model trained using the dimension-reduced FC matrices for differentiating each task condition comparison. **Right:** Instead of

defining clusters using the FCMA-then-clustering pipeline, we selected the top best 16 parcels predefined in Schaefer 1000 parcellation scheme in separating perception from retrieval states using the same cross-validation framework (**Figure S1**). We then examined the performance of models trained using FC matrices among predefined Schaefer parcels for differentiating each task condition comparison.

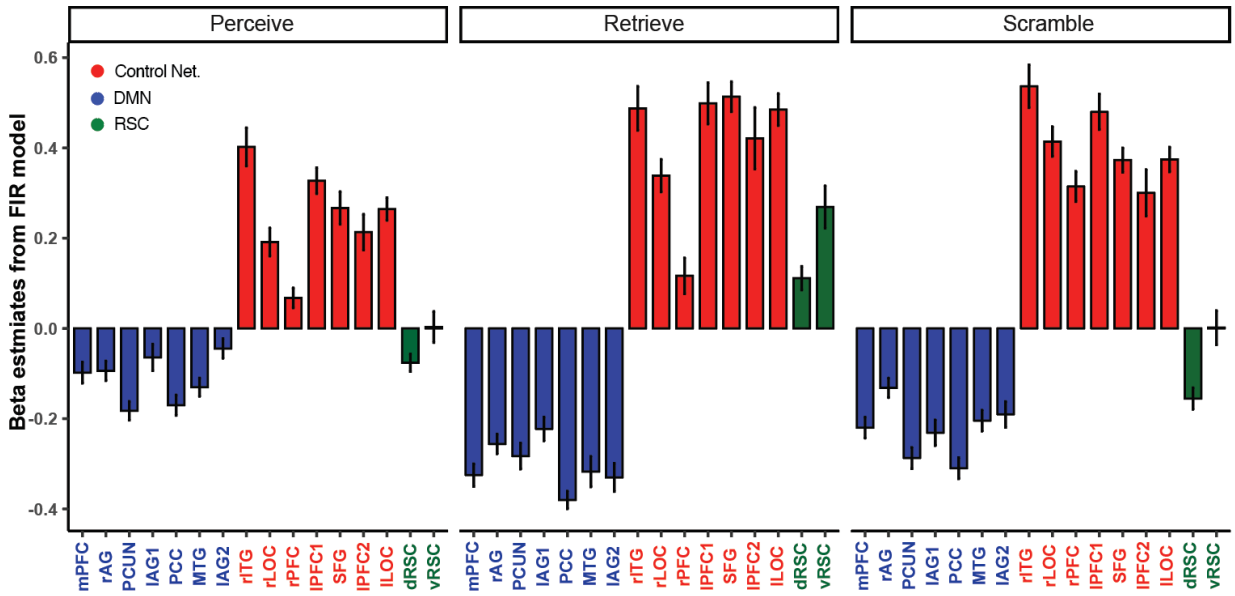


**Supplementary Figure 5**. Univariate activation profiles of the 16 clusters across 3 functional communities during each task condition. The FIR model consists of 36 (4 TR instruction + 24 TR task + 8 TR IBI) x 2 (epoch category) x 3 (condition) = 216 regressors. Thus, there are 24 (TR task) x 2 (epoch category) = 48 regressors that modeled task activations for each condition. Here for each participant, we computed the averaged beta estimates (of the 48 regressors) for all voxels within a cluster per condition. The error bar indicates the standard error of the mean of beta estimates. The color indicates the functional community assignment of each cluster.

| ClusterIdx | Brain Region | Volume | X | Y | Z | MaxInt |
|---|---|---|---|---|---|---|
| 1 | Medial prefrontal cortex | 620 | -0.5 | 44.3 | -1.0 | 9.1354 |
| 2 | R-Inferior parietal lobule | 519 | 60.1 | -26.4 | 49.0 | 8.0306 |
| 3 | Dorsal retrosplenial cortex | 400 | -18.2 | -69.3 | 24.0 | 7.8805 |
| 4 | L-Intraparietal sulcus | 377 | -33.3 | -59.2 | 41.5 | 8.2977 |
| 5 | R-Intraparietal sulcus | 364 | 29.8 | -66.8 | 36.5 | 7.0853 |
| 6 | Precuneus | 308 | -10.6 | -54.2 | 44.0 | 7.4746 |
| 7 | L-Inferior parietal lobule1 | 117 | -66.2 | -51.7 | 9.0 | 5.9631 |
| 8 | R-Lateral prefrontal gyrus | 116 | 52.5 | 9.0 | 19.0 | 6.4338 |
| 9 | L-Lateral prefrontal gyrus1 | 116 | -53.6 | 16.5 | 31.5 | 7.3036 |
| 10 | Posterior cingulate cortex | 107 | 2.0 | -18.8 | 44.0 | 7.3742 |
| 11 | Ventral retrosplenial cortex | 103 | 14.6 | -54.2 | 14.0 | 7.0643 |
| 12 | Superior frontal gyrus | 82 | -3.0 | 16.5 | 51.5 | 7.2724 |
| 13 | L-Lateral prefrontal gyrus2 | 64 | -48.5 | 29.2 | 24.0 | 6.2349 |
| 14 | Posterior middle temporal gyrus | 58 | 62.6 | -16.3 | -11.0 | 6.2996 |
| 15 | L-Inferior parietal lobule2 | 52 | -61.1 | -49.1 | 44.0 | 6.9956 |
| 16 | R-Inferior temporal gyrus | 49 | 55.1 | -56.7 | -13.5 | 5.8310 |

Table 1. Sizes and locations of the clusters of interest.

**Within- and Between-Community Background FC Discriminate Perception from Retrieval States**

Our FCMA-then-clustering pipeline successfully identified a tractable number of connections among selected brain clusters that differentiate perception from retrieval states. In the next set of analyses, we aimed to characterize these differentiating connections by examining background FC densities within- and between functional communities across the two cognitive states. To do that, for each subject we averaged across background FC matrices for each epoch within a condition, obtaining one 16 by 16 background FC matrix for each condition. We then averaged those of the *Perceive* and *Scramble* conditions to obtain a single measure of background FC for perception state for each subject. Note that we expected to observe background FC differences because the clusters were selected due to their sensitivity to state-related changes; the goal of this analysis is to interpret the difference.

We first examined the background FC densities for all cluster pairs within the same functional community during perception versus retrieval states, as previous investigations suggested that memory-related regions may show stronger coupling strengths during retrieval (Cooper & Ritchey, 2019). **Figure 4a** shows the group-level differences in cluster-to-cluster background FC density across the two states (perception – retrieval). Simple visual inspections revealed that most intra-Control network communications (17 out of 21 connections) were stronger during perception state, whereas the majority of intra-DMN connections (17 out of 21 connections) were more substantial during retrieval state (**Figure 4a**). Quantitively, a repeated measure ANOVA with factors of cognitive state (i.e., perception vs. retrieval state) and functional community (i.e., DMN, Control Net., and RSC) revealed a significant interaction between the two factors ($F_{(2, 46)} = 19.05$, $p < 0.001$, $\eta^2 = 0.45$; **Figure 4b**). This interaction suggests that the averaged background FC densities between RSC clusters and cluster pairs within the Control network were stronger during perception compared to retrieval state (RSC: $t_{(23)} = 2.94$, $p = 0.007$, 95% CI = [0.02, 0.1], Cohen's d = 0.49; Control: $t_{(23)} = 2.26$, $p = 0.03$, 95% CI = [0.01, 0.06], Cohen's d = 0.42; **Figure 4a left**) whereas those between clusters in DMN were numerically stronger during retrieval than perception state ($t_{(23)} = 1.87$, $p = 0.07$, 95% CI = [-0.06, 0.01], Cohen's d = 0.32; **Figure 4a right**). Additionally, the repeated measure ANOVA also revealed a significant main effect of functional community ($F_{(2, 46)} = 228.56$, $p < 0.001$, $\eta^2 = 0.91$). A follow-up t-test suggested that clusters within the Control network had overall stronger connectivity density compared to those within in the DMN ($t_{(23)} = 5.54$, $p < 0.001$, 95% CI = [0.05, 0.1], Cohen's d = 0.93). Note that this result holds even after accounting for the anatomical distances between clusters. On the other hand, the strong coupling strengths between RSC regions were largely due to the fact that the two RSC clusters were anatomically close to each other (**Figure S6**). Lastly, the ANOVA did not reveal a significant main effect of cognitive state ($F_{(1, 23)} = 2.06$, $p = 0.16$, $\eta^2 = 0.08$), suggesting that the overall background FC densities were comparable across perception and retrieval.

We then examined the background FC densities for cluster pairs in different functional communities across perception and retrieval states. Our results found distinct background FC patterns among clusters in the control network. Specifically, some Control clusters (e.g., rPFC) tend to couple with DMN clusters more strongly during the retrieval state, whereas other Control clusters (e.g., SFG) had stronger coupling with DMN clusters during the perception state (**Figure 4c**, **d**). Nevertheless, the averaged background FC strengths of cluster pairs in Control network and DMN were comparable across the two cognitive states ($t_{(23)}$ = 1.38, $p$ = 0.18, 95% CI = [-0.1, -0.02], Cohen's d = 0.39). Moreover, consistent with our observation in **Figure 3b**, our results suggested that RSC shifted from coupling with the Control network to DMN, as cognitive states shifted from retrieval to perception (**Figure 4e**)**.** A repeated measure ANOVA with factors of cognitive task state (i.e., perception and retrieval) and network (i.e., the averaged connectivity measure between RSC nodes and regions in either Control or DMN regions) revealed a significant interaction between the two factors ($F_{(1, 23)}$ = 100.94, $p < 0.0001$, $\eta^2$ = 0.81; **Figure 4f**). Specifically, RSC nodes had stronger averaged background connectivity strength with DMN nodes during the perception state ($t_{(23)}$ = 4.83, $p < 0.001$, 95% CI = [0.05, 0.12], Cohen's d = 0.76), but stronger background connectivity strength with Control nodes during retrieval state. ($t_{(23)}$ = 2.35, $p$ = 0.03, 95% CI = [0.01, 0.09], Cohen's d = 0.43). The ANOVA did not reveal any significant main effect of cognitive task state ($F_{(1, 23)}$ 1.22, $p$ = 0.28, $\eta^2$ = 0.05) nor network ($F_{(1, 23)}$ = 0.01, $p$ = 0.91, $\eta^2 < 0.01$).

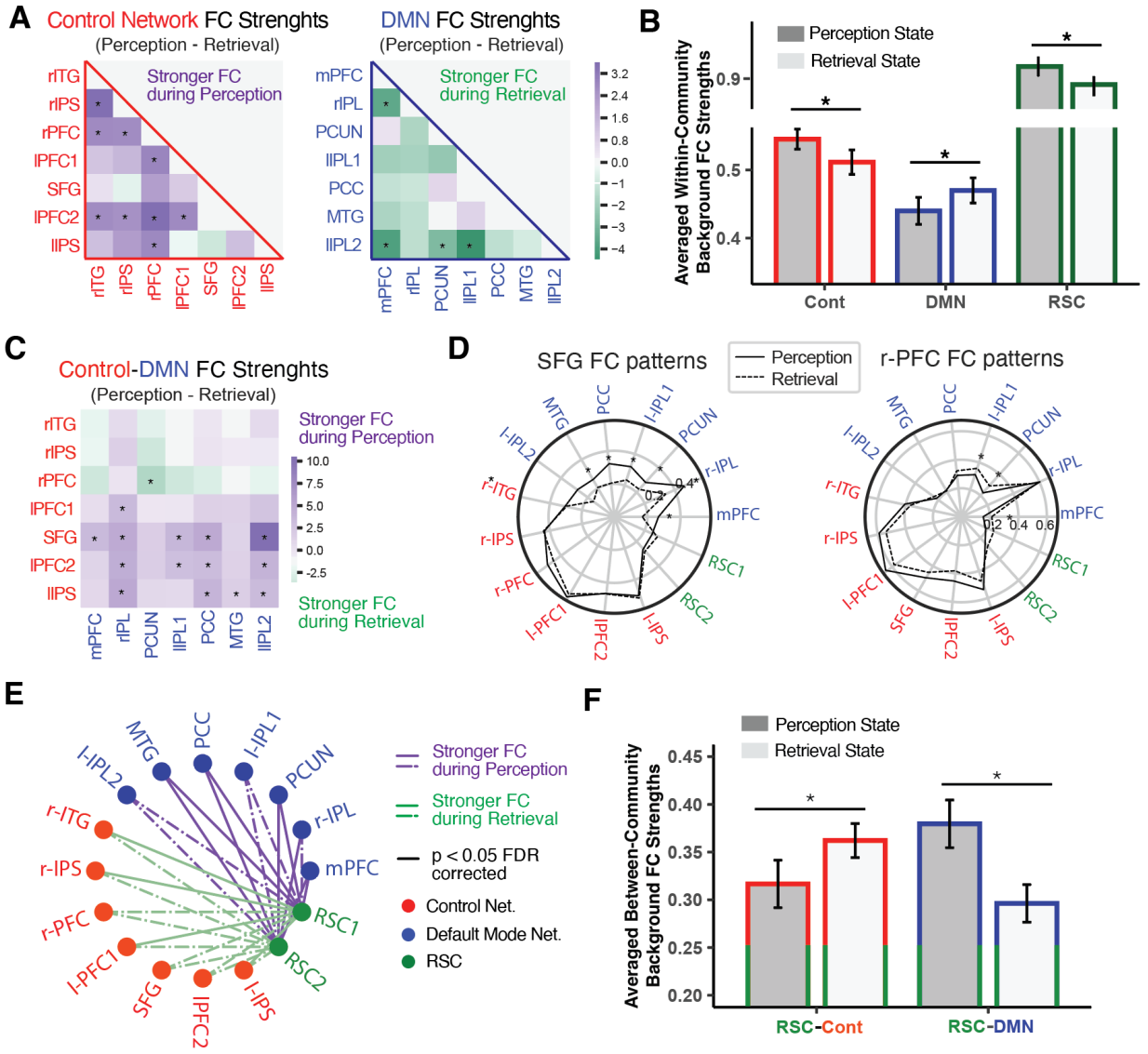


**Figure 4.** Connectivity configurations during perception and retrieval cognitive states. **A**) Group-level differences in background FC strengths between each pair of clusters (within a same functional community) across the two cognitive states (perception – retrieval). The color of each cell represents the sign and magnitude of the t values, with a positive value indicating stronger coupling during perception state and a negative value suggesting stronger coupling during retrieval state. Asterisks indicate $p < 0.05$ after FDR correction. **B**) Background FC strengths averaged across all pairwise connectivity within the same functional community across perception and retrieval states. **C**) Group-level differences in background FC strengths between pairs of clusters in different functional communities (DMN and Control network) across the two cognitive states (perception – retrieval). The color of each cell represents the sign and magnitude of the t values and asterisks indicate $p < 0.05$ after FDR correction. **D**) Background FC patterns of superior frontal gyrus (SFG) and right prefrontal cortex (rPFC) during perception and retrieval states. **E**) Group-level differences in background FC strengths between RSC clusters and

DMN/Control clusters across the two cognitive states (perception – retrieval). The color of each line represents the sign of the t values, with purple indicating stronger coupling during perception state and green suggesting stronger coupling during retrieval state. Solid lines indicate $p < 0.05$ after FDR correction. **F**) Background FC strengths averaged across all pairwise connectivity between RSC clusters and DMN/Control clusters.

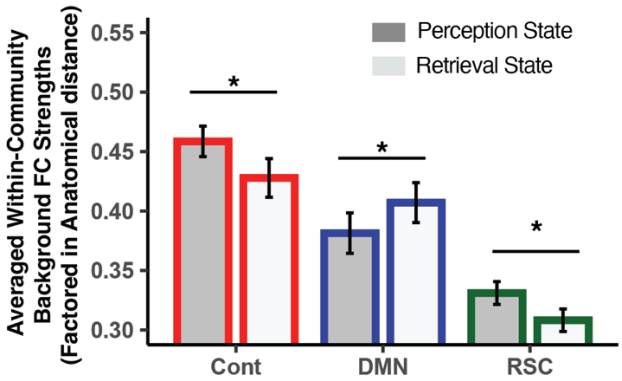


**Supplementary Figure 6.** Background FC strengths averaged across all pairwise connectivity within the same functional community across perception and retrieval states, after factoring in anatomical distance. Using MNI coordinates in **Table 1**, anatomical distance was quantified as the Euclidean distance between each pair of clusters (divided by 100 to make the y-axis unit comparable to **Figure 4b**). The adjusted background FC strengths were computed as $FC\ strength\ \times\ anatomical\ distance$, thus closer anatomical distance (e.g., the two RSC cluster) would lead to FC strengths shrinkage. After factoring in anatomical distance, clusters within the Control network still retained overall stronger connectivity density compared to those within in the DMN ($t_{(23)} = 4.03$, $p < 0.001$, 95% CI = [0.02, 0.07], Cohen's d = 0.70). On the other hand, the strong coupling strengths between RSC regions observed in **Figure 4b** could be largely attributed to the short anatomical distance between the two RSC clusters.

**Retrosplenial Cortex is Crucial for Establishing Perception and Retrieval States**

During the current experiment, participants needed to represent three distinctions to perform different conditions of the task. Specifically, they need to distinguish (1) which visual category is currently being presented (i.e., face vs. scene, **Figure 5a left**), (2) which behavioral task was instructed to perform (i.e., male/female vs. natural/manmade, **Figure 5a middle**), and (3) which cognitive state is required to complete the behavioral task given the visual category (i.e., perception vs. retrieval, **Figure 5a right**). Here, we performed pattern similarity analyses to assess how strongly each of these three distinctions was represented in each cluster (and functional community), looking separately at each cluster's background FC patterns and stimulus-evoked activity patterns. For each cluster, pattern similarities between pairs of epochs were computed (**Figure 5a**, **b**), and the averaged differences between within-class pattern similarity (e.g., face-face/scene-scene) and between-class pattern similarity (e.g., face-scene) were used to index the cluster's sensitivity to the respective distinction. We then averaged across clusters within each functional community, yielding 3 sensitivity indices for each functional network per participants (**Figure 5c**-**e**).

Pattern similarity measures of background FC suggested that clusters in different functional communities demonstrated different levels of sensitivity to cognitive states (**Figure 5c**; $F_{(2,46)} = 6.32$, $p = 0.003$, $\eta^2 = 0.22$). In particular, RSC sensitivity indices were significantly greater than the Control network ($t_{(23)} = 2.98$, $p = 0.006$, 95% CI = [0.01, 0.05], Cohen's d = 0.78) and numerically greater than the DMN ($t_{(23)} = 1.95$, $p = 0.06$, 95% CI = [-0.01, 0.04], Cohen's d = 0.49). Note that although clusters were initially selected because their background FC patterns differentiate between cognitive states, this approach was not guaranteed to observe any differences between clusters or functional communities. That is, this finding is not due to circularity in our analyses. On the other hand, pattern similarity measures of evoked activations indicated that clusters in different functional communities also showed different level of sensitivities to visual categories (**Figure 5d**; $F_{(2,46)} = 48.35$, $p < 0.001$, $\eta^2 = 0.68$) and behavioral tasks (**Figure 5e**; $F_{(2,46)} = 26.92$, $p < 0.001$, $\eta^2 = 0.54$). Importantly, the evoked activity patterns of RSC were significantly more sensitive to these two distinctions compared to those of the DMN (visual-category: $t_{(23)} = 9.02$, $p < 0.001$, 95% CI = [0.12, 0.19], Cohen's d = 2.26; behavioral-tasks: $t_{(23)} = 5.70$, $p < 0.001$, 95% CI = [0.04, 0.08], Cohen's d = 1.38) and the Control network (visual-category: $t_{(23)} = 4.52$, $p < 0.001$, 95% CI = [0.05, 0.13], Cohen's d = 1.21; behavioral-tasks: $t_{(23)} = 5.00$, $p < 0.001$, 95% CI = [0.03, 0.07], Cohen's d = 1.25). Together these pattern similarity results highlight the important role of RSC regions in establishing perception and retrieval states that support task performance.

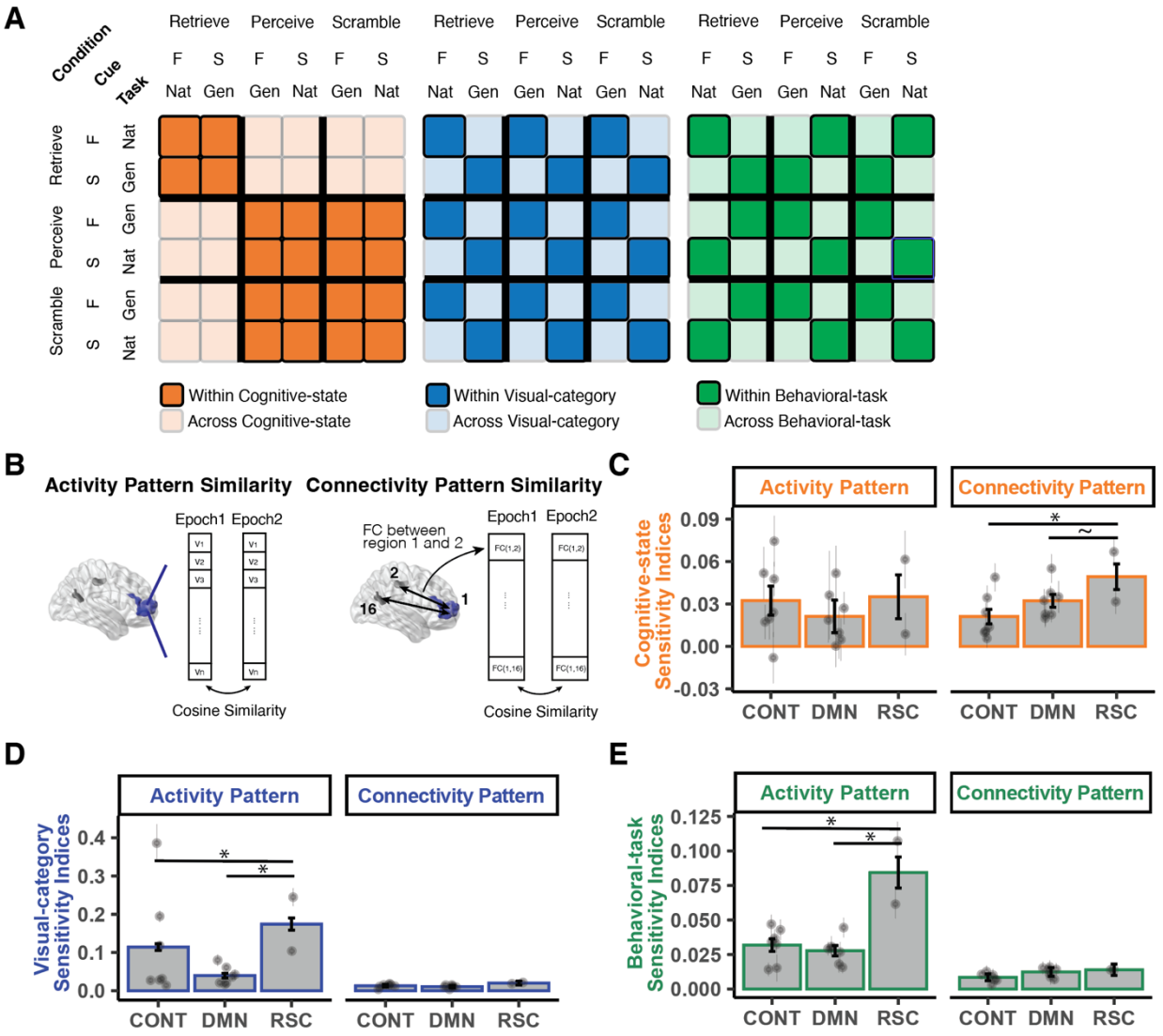


**Figure 5.** Pattern similarity analyses using both background FC patterns and stimulus-evoked activity patterns. **A**) Diagram for computing pattern similarity measures between pairs of epochs for each of the three distinctions (cognitive state, visual category, behavioral task). Darker colors indicate epochs of the same class (e.g., visual categories being face-face) whereas light colors indicate epochs of different classes (e.g., visual categories being face-scene). **B**) Diagram for computing pattern similarity measures with both FC and activity patterns. When computing activity pattern similarity measures, each epoch is represented by a *n*-dimensional vector, where *n* is the total number of voxels in the respective cluster. When computing connectivity pattern similarity, each epoch is represented by a 15-dimensional vector, representing the background FC measure between this cluster and the other 15 clusters. **C**-**E**) Sensitivity indices of each functional community with regard to each of the three distinctions. Sensitivity indices were quantified as the averaged differences between measures of within-class epoch similarity and between-class epoch similarity. Asterisks indicate $p < 0.05$

## DISCUSSION

The goal of the current study was to characterize and differentiate perception versus retrieval states in a way that respects the complexity of whole-brain functional connectivity (FC). First, we found that the stimulus-independent background FC patterns of perception versus retrieval states are systematically different (i.e., linearly separable; **Figure 2a**). Moreover, the differences were best captured by background FC patterns between 16 clusters across 3 hypothesized functional communities (**Figure 3; Table 1**). Our whole-brain analyses pipeline allowed us to extend findings from previous research (Cooper & Ritchey, 2019) by identifying important brain clusters and coupling patterns beyond memory-related brain regions (**Figure 4**). Second, our results showed that background FC and evoked activations tend to capture distinct components of the cognitive processes (**Figure 2b**), with the former being more "state-related" and the latter being more "stimulus-related" (Summerfield et al., 2006). Third, we demonstrated the utility of full correlation matrix analysis (FCMA; Kumar et al., 2022; Wang et al., 2015) and showed how the feature selection process of FCMA, paired with cluster-based dimensionality reduction, can be used to improve the interpretability of high-dimensional FC results (**Figure S1, S4**). Lastly, we discussed a perspective of aligning of our results with a framework of selective attention where, given the same perceptual input, directing attention externally would promote perception of the input-related sensory features, whereas directing attention internally would promote retrieval of the input-associated episodes (Chun et al., 2011).

### Background Functional Connectivity Configurations Underlying Perception and Retrieval States

The current study positions the same visual input as being either the target of visual perception or the trigger for episodic memory. Our results suggest that, to successfully perform tasks in different conditions, the brain engages distinct background FC configurations to maintain a sustained cognitive state for either perception or retrieval (**Figure 2a**). Similar state-related shifts in background FC configurations have been reported in previous work. Primarily focusing on a set of predefined regions of interest (ROI), Cooper and Ritchey (2019) found that regions in memory-related cortical systems (anterior temporal and parietal memory networks; Ranganath & Ritchey, 2012) showed stronger background FC during retrieval over perception. Using a purely data-driven approach, our findings are largely consistent with Cooper and Ritchey (2019), as we found that retrieval (vs. perception) state is characterized by stronger background coupling between clusters in the default mode network (DMN), which is important for internal cognitive processes (Buckner et al., 2008; Yeshurun et al., 2021). Specifically, our data-driven pipeline highlighted seven clusters in the DMN (blue clusters in **Figure 3a; Figure 4a,b**), including the bilateral inferior parietal lobule (IPL), posterior cingulate cortex (PCC), precuneus (PCUN), medial prefrontal cortex (mPFC) and middle temporal gyrus (MTG). Note that IPL, PCUN, and PCC are considered parts of the parietal memory (PM) network for memory-guided behaviors (Ranganath & Ritchey, 2012), and IPL, PCC and mPFC have been shown to form a "core recollection network", supporting memory retrieval successes

(Rugg & Vilberg, 2013). Indeed, several studies have showed that functional interactions between these regions contribute to different aspects of episodic memory (Cooper & Ritchey, 2019; Geib et al., 2017; King et al., 2015). In particular, it was proposed that the interaction between the IPL and PCUN connects episodic features to form an integrated neural representation, while conceptual knowledge and existing schemas are integrated by PCC and mPFC (Ranganath & Ritchey, 2012; Ritchey & Cooper, 2020). Moreover, our findings extend previous work by showing that the perception (vs. retrieval) state is characterized by increased background FC within a control network (red clusters in **Figure 3a; Figure 4a,b**). Specifically, this network includes the lateral bilateral prefrontal cortices (lPFC), intraparietal sulcus (IPL), inferior temporal gyrus (IT) and superior frontal gyrus (SFG). Previous research has consistently categorized these regions as a part of the task-positive or external attention system (Fornito et al., 2012; Golland et al., 2008), which is important for mediating attention to exogenous stimuli. More fine-grained brain parcellation studies have suggested these regions are part of the frontoparietal and ventral attention networks, which are important for bottom-up or reactive cognitive control processes (Braver, 2012; Gordon et al., 2016; H. Kim et al., 2010; Yeo et al., 2011). Together, our results are consistent with the idea that the brain has two global systems that are “externally-oriented” and “internally-oriented” (Golland et al., 2008; Honey et al., 2017), and the alternation between these two states leads to the transition between perception and retrieval cognitive states.

Importantly, our whole-brain data-driven approach also highlighted the importance of the background FC patterns in retrosplenial cortex (RSC; green clusters in Figure 3a) for accurately characterizing perception versus retrieval states. Specifically, we showed that RSC-DMN coupling was substantially greater during the perception state whereas RSC-Control coupling was greater during the retrieval state (**Figure 4e**, **f**). Indeed, this connectivity pattern may seem counterintuitive at first, but we argue that this finding is not in conflict with previous research. RSC is hypothesized to be part of the posterior medial (PM) network (Ranganath & Ritchey, 2012), and its background FC patterns were also examined in Cooper and Ritchey (2019). Their results suggested that, although most ROIs in the PM network showed stronger coupling with each other during retrieval compared to perception, the background FC patterns of RSC did not demonstrate observable enhancement during retrieval state with any other regions in the PM network (c.f., Figure 3c right in Cooper & Ritchey, 2019). More importantly, instead of showing stronger coupling with PM regions during retrieval state, they found that RSC had numerically stronger background FC with task-positive regions, such as the inferior temporal cortex, which is consistent with what we observed in the current study (**Figure 4e**). Benefiting from the whole-brain data-driven approach, the current study revealed a more complete picture of RSC background FC during perception and retrieval states, identifying regions in the DMN and Control networks beyond the classical memory-related systems (Cooper & Ritchey, 2019). Previous human fMRI and rodent studies suggest that RSC is involved in connecting external and internal states (Bicanski & Burgess, 2018; Yeshurun et al., 2021). For example, a

rodent study found that RSC (in mice) integrates both allocentric mapping (the animal's location in the external world) and egocentric frame (the animal's internal representation of the location) to navigate through a maze (Alexander & Nitz, 2015) by combining sensory inputs and mnemonic information from the medial temporal network (Bicanski & Burgess, 2018). Similarly, human RSC has been proposed to be a hub for connecting external and internal worlds (Yeshurun et al., 2021), such that it integrates external cues with self-generated information to guide behavior (Ranganath & Ritchey, 2012). In this respect, background FC in RSC during perception and retrieval may capture the role of RSC in bridging perceptual and mnemonic (or internally-oriented) information. Nevertheless, further investigation is needed to fully characterize how the observed background FC patterns of RSC establish the perception and retrieval states.

The current findings appear to be inconsistent with previous work suggesting that background FC patterns among hippocampal subregions contribute to separating perception and retrieval states (Bein et al., 2020; Duncan et al., 2012; Honey et al., 2017). These works showed that coupling between CA1 and CA3/DG is stronger during retrieval compared to perception states. By contrast, clusters identified in the current study did not include hippocampal subregions. We argue that this could be due to the fact that FCMA was configured to generate group-level voxel masks, ignoring individual differences in hippocampal subfield anatomy. Hippocampus is a relatively small brain region, and its subfields often include on the order of dozens of voxels (under typical scanning parameters) that may differ in their precise anatomical location across individuals. As a result, analyses of hippocampal subregions require subject-level hippocampal subfield segmentation, with each subject obtaining a slightly different segmentation map. In this respect, a shared group-level voxel mask may not be able to capture the important but subtle interactions among hippocampal subfields.

**Background FC Captures "State-Related" Signal and Activations Reflect "Stimulus-Related" Signal**

Previous work has suggested that mental states can be reflected in distributed and overlapping patterns in the brain. A major line of work has aimed to decode information carried by regional brain activation patterns using the technique referred to as multivariate pattern analysis (MVPA) (Norman et al., 2006). On the other hand, another line of complementary work has investigated the inter-regional connectivity structure of the brain by examining the temporal interaction patterns (functional connectivity; FC) between multiple brain regions (Smith, 2012). Both lines of work have been fruitful, resulting in tremendous insights into our understandings of human cognitive processes (Haxby, 2012; Song & Rosenberg, 2021). Importantly, some previous research has suggested that these two neural measures are likely to capture and reflect distinct, or at least non-overlapping aspects of cognitive processes. For example, Song et al. (2021) found that when viewing or listening to narratives, ongoing attentional engagement can only be

predicted by FC-based models, whereas models trained with regional activation patterns failed to capture this information. Additionally, Manning et al. (2018) showed that an ensemble model that relied on both and FC- and activation-based neural measures outperformed models that utilized a single type of neural measure (i.e., only FC or only activation). From a computational perspective, this result suggests that activation and FC patterns capture partially non-overlapping variance of cognitive processes. Extending these findings, the current study suggests that FC-based measures are more sensitive to differences in cognitive states whereas activation-based measures are more likely reflect differences in stimulus-related features of task. Specifically, we found that FC-based classifiers better separated task conditions that involved state-related (i.e., perception vs. retrieval) than those only involved stimulus-related differences (e.g., visual content). On the contrary, MVPA classifiers did not demonstrate a clear preference for state-related comparisons over stimulus-related distinctions (**Figure 2b**). Our findings are in line with the theory that the fMRI data acquired at each voxel are composed of both state-related and event-/stimulus-related activity, and that FC-based measures could be more better suited to capture "state-related" signals whereas activation patterns better capture the "event-related" component (Summerfield et al., 2006).

It is also worth noting that there are different types of FC-based measures; the current study primarily tested the background FC measures by regressing out the stimulus-evoked component using a general linear model (Al-Aidroos et al., 2012; Bejjanki et al., 2017; Norman-Haignere et al., 2012). However, some studies computed their FC measures without regressing out the stimulus-evoked component (e.g., Song et al., 2021), or rely on the stimulus-evoked parametric measures (e.g., beta series correlation; Bein et al., 2020). Future works could further examine whether these types of FC-based measures also preferentially capture state-related aspects of the cognitive process.

**The Utility of Feature Selection in Whole-brain Voxel-wise FC Analyses**

The current study used full correlation matrix analysis (FCMA; Kumar et al., 2022; Wang et al., 2015) to explore whether cognitive states are encoded in whole-brain voxel-wise background functional connectivity patterns. Our approach is systematically different from those used in previous studies, such as connectome-based predictive modeling (Shen et al., 2017), in two ways. First, FCMA operates on voxel-level connectivity matrices instead of the commonly-used, lower-dimensional parcel-averaged time series. Second, FCMA uses a nested leave-one-subject-out cross validation framework that enables more efficient feature selection to reduce large connectivity matrix to a tractable size. Here we discuss the potential trade-off regarding these two distinctions. First, our results suggest that FCMA identified regions that, even after clustering over contiguous voxels, retained a higher sensitivity for differences in cognitive states compared to parcel-level analyses (**Figure S4b right**). This finding is consistent with previous research suggesting that voxel-/vertex-level FC patterns are more sensitive to measures of intelligence compared to relatively coarse-grained parcel-level analysis (Feilong et al., 2021). The differences in

sensitivity could be due to the fact that many parcellation schemes were defined from whole-brain resting-state functional connectivity profiles. Yet previous work has suggested that the functional architecture of the brain might change across resting and task states (Cole et al., 2014), and may also vary across task states (Krienen et al., 2014). It is worth mentioning that the use of predefined parcellation schemes can significantly improve sensitivity (as measured by effect size) in other types of analyses (e.g., univariate analyses) compared to voxel-/vertex-level analysis (Li et al., 2021). Thus, future studies need to further investigate the use cases for predefined parcellation schemes in connectivity analyses.

Secondly, machine learning models often face the trade-off between prediction accuracy and model interpretability (Feilong et al., 2021). In the context of FC-based models, previous work has primarily focused on constructing a model for making the most accurate predictions on trait-like demographic variation (Finn et al., 2015), behavioral performance (Rosenberg et al., 2016, 2020), or task conditions (Gonzalez-Castillo et al., 2015; Shirer et al., 2012). Despite high prediction accuracies in these models, it is often hard to interpret the FC configuration given the vast number of connections. For example, Rosenberg et al. (2016) identified a high-attention network, consisted of 757 edges across the entire brain, whose connectivity strengths reliably predict better sustained attention performances. Indeed, the FC configuration profile for attentional states has a distributed nature, but is it feasible to sacrifice some degree of prediction accuracy by constraining the number of edges such that the resulting FC configuration can be more easily interpreted? The current study attempted to do this by combining a whole-brain voxel-level FC model with feature selection using a nested cross validation framework. Specifically, we quantified the "utility" of each connection using the machine learning training and testing framework (See **Method**: ***Full Correlation Matrix Analysis on Residual Activity***; **Figure S1**). As a result, we were able to select the most useful connections in an unbiased, automated fashion, reducing large correlation matrices to a tractable size. We show that models based on 120 unique edges among only a set of 16 regions were able to reach around 75% prediction accuracy when decoding cognitive states of perception and retrieval. Thus, the current study demonstrates the utility of feature selection in FC pattern-based models in order to yield the most relevant and interpretable FC configuration profile while largely maintaining prediction performance.

**Perception Versus Retrieval as Outcomes of Selective Attention**

Reconfiguration of background FC patterns has been most commonly examined as a neural mechanism underlying and result from selective attention (Desimone & Duncan, 1995). Specifically, the "switching-train-track" framework for selective attention argues that selective attention prioritizes goal-relevant information by strengthening the interaction (as measured by the changes in background FC) between goal-relevant brain regions (Al-Aidroos et al., 2012; Miller & Cohen, 2001; Turk-Browne, 2013). For example, previous work has shown that, when presented with face-scene composite stimuli, early visual

cortex shows stronger intrinsic FC coupling with face-specialized regions (e.g., fusiform area) when participants attended to the face component but with scene-specialized regions (e.g., parahippocampal place area) when participants attended to scene component (Al-Aidroos et al., 2012; Córdova et al., 2016; Norman-Haignere et al., 2012). Here we investigate perception versus retrieval states as an effect of selective attention. Specifically, a recent taxonomy dichotomized attention into external attention, with the target being perceptual information and internal attention, with the target being self-generated trains of thoughts (Chun et al., 2011). Under this dichotomy, perception versus retrieval can be thought of as a form of external vs. internal attention states for information processing. When a given input is being attended externally, the sensory information of the input is being preferentially processed while the mnemonic information is suppressed. On the other hand, when the same input cues internally-directed attention, the mnemonic information will be enhanced while the sensory information is suppressed (Chun et al., 2011; Gazzaley & Nobre, 2012). The switching-train-track account of selective attention has been mostly studied by examining FC changes within the ventral visual stream when participants were attending to different visual categories (e.g., face vs. scene). The current study has provided evidence that this account of selective attention can be potentially generalized to a whole-brain scope and to examine more complex cognitive states (e.g., perception vs. retrieval). In particular, although previous research studying perception vs. retrieval has focused primarily on decoding the "train of thoughts" (i.e., stimulus-related features; Rissman & Wagner, 2012), the selective attention perspective highlights the importance of investigating state-specific "train tracks"—i.e., background FC patterns—and understanding how such train tracks establish and sustain particular cognitive states.

## METHODS

### Participants

Thirty-three adults with normal or corrected-to-normal vision were recruited to participate for monetary compensation at Princeton University. Twenty-seven subjects who met the behavioral training criteria completed the follow-up fMRI scan and three subjects were excluded due to excessive head motion. This leaves 24 subjects in the current study (eleven reported male, mean age = 23.3 years). The Princeton University Institutional Review Board approved the study protocol, and all subjects provided informed consent. The sample size was selected based on previous studies that examined functional connectivity changes with memory (Cooper & Ritchey, 2019) and used FC patterns to differentiate task states (Shirer et al., 2012).

### Materials

Stimuli consisted of 64 scene and 64 face images. The scene images were collected from the "Massive Memory" dataset (Konkle et al., 2010; http://konklab.fas.harvard.edu/#). The face images were obtained

from the FEI face database (Thomaz & Giraldi, 2010; https://fei.edu.br/~cet/facedatabase.html) and the selected faces are of emotionally neural expressions. Scrambled images were generated as the weighted average between the actual image and its phase-scrambled version (Oppenheim & Lim, 1981; Stojanoski & Cusack, 2014). The script for creating the phase-scrambled images was adopted from https://github.com/rordenlab/spmScripts/blob/master/bmp_scramble.m.

**Procedure**

During the training phase (~20-30 minutes prior to scanning), participants were over-trained to learn associations between face and scene images on a 2-alternative forced choice test until they have correctly identified each association twice (i.e., choosing the correct face given a scene and choosing the correct scene given a face). While scanning, participants completed 3 task conditions across 6 functional runs using a block design (2 runs for each condition). Each run started with a 6-s blank lead-in period, followed by 8 task epochs and ended with a 6-s lead-out period. Each task epoch consisted of a 4-s presentation of instructions, followed by 8 2-s presentations of distinct visual cue stimuli separated by a 1-s interstimulus interval, followed by a 12-s inter-block-interval. Button-responding was only allowed during the 2-s presentation of the visual cues. Together, the duration of each trial, epoch, and run was 3 s, 40 s and 332 s, respectively.

In the *Perceive* task condition, participants were asked to identify the visual features of each cue on the screen. That is, if a face cue was presented, participants were expected to make a perceived male/female judgment of the face via a button box, whereas if a scene cue was shown, participants were expected to make perceived natural/man-made judgment of the scene. On the other hand, during the *Retrieve* task condition, participants were asked to judge the gender or naturalness of the cue-associated image (i.e., the pair of the cue from the training phase). That is, if a face cue was shown, participants needed to retrieve the face-associated scene image and make a retrieved natural/man-made decision. Likewise, if a scene cue was shown, participants were supposed to retrieve the scene-associated face image and make a retrieved male/female decision. To assure that the neural correlates we later identified were not driven by differences in task difficulties (as measured by performance accuracies) between *Perceive* and *Retrieve* task conditions, we included a *Scramble* condition, in which participants were required to perform the same perception task but with greater cognitive demands. During the *Scramble* condition, participants completed the same task as they did in the *Perceive* condition, but the visual cues were scrambled using a weighted average of the original image and its phase-scrambled version. The scramble-degree was set based on a behavioral pilot study of the same design in order to match the performance accuracy between the *Scramble* and *Retrieve* task conditions (**Figure 1**).

**Image Acquisition and Preprocessing**

The fMRI data were acquired with a 3T scanner (Siemens Prisma) at the Princeton Neuroscience Institute. Functional data were acquired using a T2*-weighted multiband EPI sequence (repetition time = 1 s, echo time = 26 ms, flip angle = 50°, FOV = 260 x 260, resolution = 2.5 x 2.5 x 2.5 mm, multiband acceleration factor = 4) with 44 axial slices aligned to the anterior commissure/posterior commissure. A whole-brain T1-weighted MPRAGE 3D anatomical volume (1 x 1 x 1 mm voxels) was collected to improve registration. One phase and two magnitude field maps were collected to correct field inhomogeneities.

The first 6 lead-in volumes of each functional run were manually discarded before entering the preprocessing pipeline. Image preprocessing was performed using fMRIPrep 20.1.0rc1 (Esteban et al., 2019). All functional images were corrected for slice-acquisition time, head motion, and susceptibility distortion, and were normalized to a standard template, yielding preprocessed BOLD runs in MNI152NLin2009cAsym space. Following fMRIPrep, the minimally preprocessed functional runs were further processed using FSL (Woolrich et al., 2001) with a Nipype implementation (Gorgolewski et al., 2011). All functional images were smoothed with a 5.0 mm FWHM Gaussian kernel and high-pass filtered at 0.01 Hz. For each subject, the 6 functional runs were then normalized using the mean and standard deviation of the resting period for each run. The resting period for each functional run was defined as the 6 lead-out volumes plus all 12-s inter-block intervals of that run, which were shifted for 4 TRs to account for the hemodynamic delay. This normalization is intended to remove the BOLD signal differences across runs and thus all 6 runs were then concatenated to one time series and used for further modeling.

**Stimulus-Evoked and Residual Activity**

We computed residual activity by regressing out the stimulus-evoked component from the preprocessed data in order mitigate stimulus-evoked coactivation confounds (Al-Aidroos et al., 2012; Cole et al., 2019). First, we constructed a confound regression model using FSL (implemented in NiPype) in order to minimize the effect of the following confound variables (obtained from fMRIPrep): six head motion parameters and the mean time series from white matter and cerebrospinal fluid. The resulting timeseries data are referred to as the stimulus-evoked activity timeseries in all subsequent analyses, as they are fully preprocessed, yet contain the stimulus-evoked components. Second, we estimated and removed the stimulus-driven components from the stimulus-evoked timeseries using a finite impulse response (FIR) model, which modeled the first 36 TRs for every epoch separately for face and scene epochs, resulting in 36 (TR) x 2 (epoch category) x 3 (condition) = 216 regressors. FIR is believed to be the optimal GLM for removing stimulus-evoked response because it does not assume the shape of the hemodynamic response function (Cole et al., 2019; Norman-Haignere et al., 2012). The residual timeseries data are referred to as the residual activity, and used for computing background FC for all subsequent analyses.

**Full Correlation Matrix Analysis on Residual Activity**

We utilized full correlation matrix analysis (FCMA) as implemented in the Brain Imaging Analysis Kit (BrainIAK; version 0.11; http://brainiak.org) to conduct an unbiased, whole-brain voxel-wise FC analysis that systematically considers all pairwise correlations in the brain to explore the differences in connectivity configurations between perception and retrieval states (Kumar et al., 2022; Wang et al., 2015). FCMA took in the residual activity and computed a full correlation matrix (i.e., whole-brain voxel-wise correlation matrix; 92745 voxels x 92745 voxels) for each task epoch. Therefore, for each subject, 8 (epoch) x 2 (run) = 16 full correlation matrices were computed per task condition (i.e., *Perceive*, *Retrieve* and *Scramble*; **Figure 1 c-e**). Using these full correlation matrices, FCMA aimed to ($i$) examine whether perception (*Perceive* and *Scramble*) versus retrieval (*Retrieve*) states can be successfully decoded from background connectivity patterns, and ($ii$) identify the connectivity configuration that characterizes each cognitive task state. FCMA achieved these goals by implementing a nested leave-one-subject-out cross-validation (LOOCV) framework. Specifically, the outer loop contains 23 training subject and 1 left-out test subject for each outer-loop iteration; and the inner loop selects 22 training subjects within the outer training set for each inner-loop iteration. Importantly, the inner loop intends to select the top K most useful voxels (based on their connectivity patterns) from the training data (**Figure S1**) and the outer loop aims to train classifiers on connectivity patterns of the selected voxels and test their performances of (**Figure 1 g, h**). Note that we also performed parcel-level analysis to demonstrate the sensitivity advantage of our more fine-grained approach. We utilized the MNI version of the Schaefer parcellation scheme (https://github.com/ThomasYeoLab/CBIG/tree/master/stable_projects/brain_parcellation/Schaefer2018_LocalGlobal/Parcellations/MNI; Schaefer et al., 2018), and performed analyses on parcellations of different granularity (400 and 1000 parcels), which yielded comparable patterns of results.

For each iteration, the inner loop worked with the training data from 23 subjects (n-1 subjects) and performed a separate, nested LOOCV on the training set. In an unbiased manner, the inner-loop tested the accuracy of using each voxel's seed maps (i.e., how this voxel is connected to the other voxels in the brain) to differentiate perception (i.e., *Perceive* and *Scramble*) from retrieval (i.e., *Retrieve*) state (**Figure S1**). Specifically, each voxel would get an accuracy score for separating *Retrieve* and *Perceive* FC patterns, and another score for separating *Retrieve* and *Scramble* FC patterns. The minimum score of the two was assigned to the voxel and all assigned scores were averaged across the inner-loop LOOCV iterations. The minimum score was used here to make sure one of the two comparisons does not drive the overall effect. For example, a voxel's seed map might be able to separate *Retrieve* from *Scramble* well by picking up the visual content information (i.e., scramble vs. intact), but not separate *Retrieve* from *Perceive* well when the visual content difference was absent. Computing the minimum accuracy scores allowed us to more accurately measure how well each voxel's seed map encoded cognitive task state differences.

The resulting scores indicated the utility of each voxel in differentiating perception from retrieval states independent of the testing data. Based on these scores, masks of the top *K* most useful voxels were created from each inner-loop and the whole-brain full correlation matrices were reduced to *k* x *k* correlation matrices. The current study tested all results with *k* = 100, 1000, 3000, 5000, 7000, 10000 and 15000 voxels, and reported the results on *k* = 3000. There are two main reasons to report our main results using the top 3000 voxels. First, model performances dramatically improved as the voxel masks were enlarged from *k* = 100 to *k* = 3000. However, the model performances seemed to plateau when the top 3000 voxels were selected. Second, our information mapping pipeline (See **Methods: *Information Mapping***) identified a shared mask that included about 3500 voxels. The results from k = 3000 therefore provides the most direct comparison and is the most relevant for subsequent analyses. Using these *k* x *k* connectivity matrices, the FCMA outer-loop trained 3 classifiers (one for each pair of task conditions, e.g., *Perceive* vs. *Retrieve*) and tested the model performance using the left-out testing data.

**Regular and Generalization Tests**

Classifiers were first trained and tested on the same task condition comparison. To quantify and compare model performance for each task comparison, we computed the area under the receiver operating characteristic curve (AUC) for each classifier. One way ANOVA was used to compare the AUCs for the three classifiers. The goals of the regular tests were to examine $(i)$ whether task conditions could be successfully decoded from background connectivity patterns and $(ii)$ whether task condition comparisons that involve cognitive task state differences (e.g., *Retrieve* vs. *Perceive*) could be decoded with higher accuracies relative to the comparison that did not involve such differences (e.g., *Scramble* vs. *Perceive*).

During the generalization test, a classifier was trained on one task condition comparison (e.g., *Perceive* vs. *Retrieve*) but tested on a different comparison (e.g., *Perceive* vs. *Scramble*). The generalization test can be conducted between each pair of task condition comparisons; we argue that the bidirectionally averaged generalization AUCs should indicated the classifiers' sensitivity to a certain type of information (**Figure 2d**). For example, both the *Retrieve* vs. *Perceive* and *Retrieve* vs. *Scramble* comparisons involve cognitive task state differences. As a result, high bidirectionally averaged AUC scores across classifiers trained on *Retrieve* vs. *Perceive* comparison while tested on *Retrieve* vs. *Scramble* comparison and classifiers trained on *Retrieve* vs. *Scramble* comparison while tested on *Retrieve* vs. *Perceive* comparison would indicate that the classifiers were indeed trained to pick up on cognitive task state information. On the other hand, high bidirectionally averaged AUC score across *Retrieve* vs. *Perceive* and *Scramble* vs. *Perceive* comparisons would suggest that the classifiers were trained to pick up on task difficulty differences. Likewise, high bidirectionally averaged AUC scores across *Scramble* vs. *Perceive* and *Scramble* vs. *Retrieve* comparisons would suggest that the classifiers were trained to detect visual features. Thus, the averaged bidirectional generalization accuracies served as information indices

measuring the degree to which the classifiers were trained to detect differences in cognitive task states, task accuracies, and visual intactness, respectively. The goal of the generalization test is to examine whether classifiers were trained to selectively detect connectivity patterns underlying perception versus retrieval task state differences.

**Multivoxel Pattern Classification Analyses**

Pattern classification analyses were performed using a support vector classifier (C = 1) implemented in the Scikit-learn module in Python (Pedregosa et al., 2011). We performed pattern classification using both the residual and the stimulus-evoked activities (See section: ***Task Evoked and Residual Activity***). First, using the *K* voxel masks generated by FCMA inner loop (See section: ***Full Correlation Matrix Analysis on Residual Activity***), we trained pattern classifiers using residual activity to perform the regular tests (i.e, train and test a model with the same task condition comparison; **Figure S2**). This analysis aims to test whether FCMA classifier performances were driven by any coactivation confounds left in the residual activity. Second, with each set of K voxel masks, we also trained pattern classifiers using stimulus-evoked activity to perform the regular test (**Figure 2b middle**). This analysis aimed to examine whether simple MVPA and background FC patterns rely on the same type of cognitive processes.

**Information Mapping**

Due to the leave-one-out cross-validation scheme, each fold of the outer-loop produced non-identical sets of voxels. To obtain a common mask, we combined the FCMA inner loop with non-parametric permutation tests to generate a group-level mask that includes all voxels that can differentiate perception from retrieval states better than chance. We obtained this group-level mask in three steps. First, we averaged the classification accuracy composite score (i.e., the minimum of the accuracy scores for separating *Retrieve* vs. *Perceive* and *Retrieve* vs. *Scramble* FC patterns) for each voxel across 24 voxel maps (**Figure S1**; one for each cross-validation fold) as the observed score. Second, we shuffled the labels of all three task conditions for each subject and repeated the outer-loop training-testing pipeline using the shuffled labels for 100 iterations. As a result, we generated a null distribution of the classification accuracy composite scores for each voxel. Using the mean and standard deviation of the classification accuracy score null distribution for each voxel, we z-transformed the observed feature selection score computed above (i.e., the group-averaged composite accuracy score). We chose a relatively stringent voxel-wise primary threshold ($P < 0.0001$) to control for false positive rates and to avoid finding large voxel clusters that span the brain (Woo et al., 2014). Voxels that passed the threshold were divided into clusters using 3dClusterize and the corresponding cluster-extent threshold was computed using 3dClustSim with AFNI (whole-volume alpha-values: -athr < 0.01). In total, 62 clusters passed the cluster-extent threshold, with size ranging from 620 to 2 voxels. In the last phase of the information mapping, we selected clusters according to their size and whether they improve model performance. Specifically, we

began with the largest cluster (620 voxels), then we sequentially added voxels from the next largest cluster to our mask and used the FCMA outer loop to test how well this set of voxels differentiated perception from retrieval states. In other words, we iteratively built a set of models, and measured the change in classification performance as the mask accumulated each new cluster of voxels (**Figure S4a**). The rationale for performing cluster selection is to identify "sufficient" nodes of the network dynamics that capture the differences between perception and retrieval states so that we could exclude the overly small clusters, and thus increase the sparsity of the identified neural correlates.

**Community Detection**

We averaged across all voxels within each cluster to obtain cluster-level time series data for each epoch. Cluster-level background functional connectivity (FC) matrices were then computed for each epoch for every subject, and then averaged within each task condition, resulting in one group-averaged connectivity matrix for the *Perceive*, *Scramble* and *Retrieve* conditions respectively. Community detection on weighted graphs was performed using the Louvain algorithm via NetworkX in Python. Following the approach used in prior work (Barnett et al., 2021; Ji et al., 2019), we ran the algorithm 1000 times on weighted graphs to tune the resolution parameter in order to maximize modularity, which describes how well a network can be subdivided into non-overlapping groups (Rubinov & Sporns, 2011). The tuned resolution parameters (gamma) were 1.10, 1.13, 1.19, for Perceive, Retrieve and Scramble task conditions, respectively. To visualize intra- and intramodular connectivity, we used the Fruchterman-Reingold force-directed projection implemented in NetworkX to project the graphs onto 2D spaces.

**Within- and Between-Communities Connectivity**

We computed a subject-level FC matrix for each task condition. We averaged the FC matrices for *Perceive* and *Scramble* conditions to create composite matrices that reflect FC dynamics underlying the perception state. To examine the coupling pattern of RSC nodes, we averaged across the connectivity strength between RSC nodes and either the DMN or the Control network clusters using both perception and retrieval state FC matrices. A two-way repeated measure ANOVA was then used to examine whether RSC nodes changed their coupling pattern with respect to the DMN and Control network nodes. To examine within-community connectivity strength, we averaged the connectivity strength between all nodes within the DMN, Control, and RSC regions for both perception and retrieval states. Similarly, a two-way repeated measure ANOVA was used to assess whether a functional community was biased toward a certain cognitive task state. All statistical analyses were performed using Pingouin 0.5.1 with Python3.

**Pattern Similarity Analyses on Stimulus-evoked Activities**

The goal of this set of analyses was to identify any potential differences between the three functional communities in their roles in performing cognitive tasks. We focused on three different cognitive aspects

and tested the degree to which each functional community was sensitive to $(i)$ the current visual categories (i.e., face vs. scene), $(ii)$ the current behavioral tasks (i.e., gender vs. naturalness judgement), and $(iii)$ current cognitive state (i.e., perception or retrieval state). To do that, we performed pattern similarity analyses using both stimulus-evoked activity patterns and background connectivity patterns.

To obtain the stimulus-evoked activity patterns, we extracted the 24 task TRs for each epoch (after being shifted 4 s to account for hemodynamic delay) from the post-confound regression time-series. These stimulus-evoked estimates were then averaged along the time dimension and reshaped into a vector for each cluster (length of the vector is the number of voxels in that cluster). On the other hand, background connectivity patterns for each cluster were computed as the temporal correlation between this cluster and other 15 clusters, reshaped into a 15-dimensional vector for each ROI (**Figure 5b**). To compute pattern similarity measures, the Fisher's Z transformed correlations between each pair of vectors from different functional runs were calculated (Kriegeskorte et al., 2009; **Figure 5a**). Sensitivity was quantified as the difference between within-state epoch pattern similarity and between-state epoch pattern similarity. For example, when examining sensitivities for the current task goal, pattern similarities were computed among all epochs within same task states (i.e., gender/gender and naturalness/naturalness) and all epochs between the two visual states (i.e., gender/naturalness). Task-state sensitivity was calculated by using the averaged within-state pattern similarity score minus the averaged between-states pattern similarity score. Thus, a significantly positive sensitivity index would suggest that the given ROI was engaged in distinct activity and/or connectivity patterns for the two task goals. We averaged the sensitivity scores across ROIs within the same functional communities. A one-way ANOVA was used to compare sensitivity scores of each cognitive process across the three functional communities.

**Data and Code Availability**

Processed fMRI data including both the stimulus-evoked and residual time series supporting the primary findings of this study are available on the Open Science Framework (OSF) at https://osf.io/yfwc7/. Scripts for performing and reproducing the specific analyses described in this paper can be found through Github at https://github.com/peetal/Decode_AttenStates.

**Funding and Acknowledgement**

This work was supported by ???. We express our deepest thanks for the feedback we have received from Dr. Ken Norman and Dr. Sam Nastase. We are also grateful for helpful discussions and supports from members of the Hutchinson Lab of Cognitive Neuroscience, the Dubrow Lab, and the Kuhl Lab.

**Credit Authorship Contribution Statement**

Study conception and design: Yida Wang, Nicholas B. Turk-Browne, J. Benjamin Hutchinson

Data Collection: J. Benjamin Hutchinson

Analysis and interpretation of results: Y. Peeta Li, Brice A. Kuhl[1], J. Benjamin Hutchinson

Draft manuscript preparation: Y. Peeta Li, Brice A. Kuhl[1], J. Benjamin Hutchinson

**REFERENCES**

Al-Aidroos, N., Said, C. P., & Turk-Browne, N. B. (2012). Top-down attention switches coupling between low-level and high-level areas of human visual cortex. *Proceedings of the National Academy of Sciences*, *109*(36), 14675–14680. https://doi.org/10.1073/pnas.1202095109

Alexander, A. S., & Nitz, D. A. (2015). Retrosplenial cortex maps the conjunction of internal and external spaces. *Nature Neuroscience*, *18*(8), 1143–1151. https://doi.org/10.1038/nn.4058

Barnett, A. J., Reilly, W., Dimsdale-Zucker, H. R., Mizrak, E., Reagh, Z., & Ranganath, C. (2021). Intrinsic connectivity reveals functionally distinct cortico-hippocampal networks in the human brain. *PLoS Biology*, *19*(6), e3001275–e3001275. https://doi.org/10.1371/journal.pbio.3001275

Beckmann, C. F., DeLuca, M., Devlin, J. T., & Smith, S. M. (2005). Investigations into resting-state connectivity using independent component analysis. *Philosophical Transactions of the Royal Society of London. Series B, Biological Sciences*, *360*(1457), 1001–1013. https://doi.org/10.1098/rstb.2005.1634

Bein, O., Duncan, K., & Davachi, L. (2020). Mnemonic prediction errors bias hippocampal states. *Nature Communications*, *11*(1), 3451. https://doi.org/10.1038/s41467-020-17287-1

Bejjanki, V. R., Silveira, R. A. da, Cohen, J. D., & Turk-Browne, N. B. (2017). Noise correlations in the human brain and their impact on pattern classification. *PLOS Computational Biology*, *13*(8), e1005674. https://doi.org/10.1371/journal.pcbi.1005674

Bicanski, A., & Burgess, N. (2018). A neural-level model of spatial memory and imagery. *ELife*, *7*, e33752. https://doi.org/10.7554/eLife.33752

Blondel, V. D., Guillaume, J.-L., Lambiotte, R., & Lefebvre, E. (2008). Fast unfolding of communities in large networks. *Journal of Statistical Mechanics: Theory and Experiment*, *2008*(10), P10008. https://doi.org/10.1088/1742-5468/2008/10/P10008

Bosch, S. E., Jehee, J. F. M., Fernández, G., & Doeller, C. F. (2014). Reinstatement of associative memories in early visual cortex is signaled by the hippocampus. *The Journal of Neuroscience: The Official Journal of the Society for Neuroscience*, *34*(22), 7493–7500. https://doi.org/10.1523/JNEUROSCI.0805-14.2014

Braun, U., Schäfer, A., Walter, H., Erk, S., Romanczuk-Seiferth, N., Haddad, L., Schweiger, J. I., Grimm, O., Heinz, A., Tost, H., Meyer-Lindenberg, A., & Bassett, D. S. (2015). Dynamic reconfiguration of frontal brain networks during executive cognition in humans. *Proceedings of the National Academy of Sciences*, *112*(37), 11678–11683.

Braver, T. S. (2012). The variable nature of cognitive control: A dual mechanisms framework. *Trends in Cognitive Sciences*, *16*(2), 106–113. https://doi.org/10.1016/j.tics.2011.12.010

Buckner, R. L., Andrews-Hanna, J. R., & Schacter, D. L. (2008). The Brain's Default Network. *Annals of the New York Academy of Sciences*, *1124*(1), 1–38. https://doi.org/10.1196/annals.1440.011

Carrasco, M., Ling, S., & Read, S. (2004). Attention alters appearance. *Nature Neuroscience*, *7*(3), 308–313. https://doi.org/10.1038/nn1194

Chun, M. M., Golomb, J. D., & Turk-Browne, N. B. (2011). A Taxonomy of External and Internal Attention. *Annual Review of Psychology*, *62*(1), 73–101. https://doi.org/10.1146/annurev.psych.093008.100427

Cole, M. W., Bassett, D. S., Power, J. D., Braver, T. S., & Petersen, S. E. (2014). Intrinsic and Task-Evoked Network Architectures of the Human Brain. *Neuron*, *83*(1), 238–251. https://doi.org/10.1016/j.neuron.2014.05.014

Cole, M. W., Ito, T., Schultz, D., Mill, R., Chen, R., & Cocuzza, C. (2019). Task activations produce spurious but systematic inflation of task functional connectivity estimates. *NeuroImage*, *189*, 1–18. https://doi.org/10.1016/j.neuroimage.2018.12.054

Cooper, R. A., & Ritchey, M. (2019). Cortico-hippocampal network connections support the multidimensional quality of episodic memory. *ELife*, *8*, e45591. https://doi.org/10.7554/eLife.45591

Córdova, N. I., Tompary, A., & Turk-Browne, N. B. (2016). Attentional modulation of background connectivity between ventral visual cortex and the medial temporal lobe. *Neurobiology of Learning and Memory*, *134*, 115–122. https://doi.org/10.1016/j.nlm.2016.06.011

Desimone, R., & Duncan, J. (1995). Neural Mechanisms of Selective Visual Attention. *Annual Review of Neuroscience*, *18*, 193–222. https://doi.org/10.1146/annurev.ne.18.030195.001205

Duncan, K., Sadanand, A., & Davachi, L. (2012). Memory's Penumbra: Episodic Memory Decisions Induce Lingering Mnemonic Biases. *Science*, *337*(6093), 485–487. https://doi.org/10.1126/science.1221936

Duncan, K., Tompary, A., & Davachi, L. (2014). Associative Encoding and Retrieval Are Predicted by Functional Connectivity in Distinct Hippocampal Area CA1 Pathways. *Journal of Neuroscience*, *34*(34), 11188–11198. https://doi.org/10.1523/JNEUROSCI.0521-14.2014

Esteban, O., Markiewicz, C. J., Blair, R. W., Moodie, C. A., Isik, A. I., Erramuzpe, A., Kent, J. D., Goncalves, M., DuPre, E., Snyder, M., Oya, H., Ghosh, S. S., Wright, J., Durnez, J., Poldrack, R. A., & Gorgolewski, K. J. (2019). fMRIPrep: A robust preprocessing pipeline for functional MRI. *Nature Methods*, *16*(1), 111–116. https://doi.org/10.1038/s41592-018-0235-4

Favila, S. E., Kuhl, B. A., & Winawer, J. (2020). Perception and memory have distinct spatial tuning properties in human visual cortex. *BioRxiv*, 811331. https://doi.org/10.1101/811331

Feilong, M., Guntupalli, J. S., & Haxby, J. V. (2021). The neural basis of intelligence in fine-grained cortical topographies. *ELife*, *10*, e64058. https://doi.org/10.7554/eLife.64058

Finn, E. S., Shen, X., Scheinost, D., Rosenberg, M. D., Huang, J., Chun, M. M., Papademetris, X., & Constable, R. T. (2015). Functional connectome fingerprinting: Identifying individuals using patterns of brain connectivity. *Nature Neuroscience*, *18*(11), 1664–1671. https://doi.org/10.1038/nn.4135

Fornito, A., Harrison, B. J., Zalesky, A., & Simons, J. S. (2012). Competitive and cooperative dynamics of large-scale brain functional networks supporting recollection. *Proceedings of the National Academy of Sciences*, *109*(31), 12788–12793. https://doi.org/10.1073/pnas.1204185109

Fruchterman, T. M. J., & Reingold, E. M. (1991). Graph drawing by force-directed placement. *Software: Practice and Experience*, *21*(11), 1129–1164. https://doi.org/10.1002/spe.4380211102

Gazzaley, A., & Nobre, A. C. (2012). Top-down modulation: Bridging selective attention and working memory. *Trends in Cognitive Sciences*, *16*(2), 129–135. https://doi.org/10.1016/j.tics.2011.11.014

Geib, B. R., Stanley, M. L., Dennis, N. A., Woldorff, M. G., & Cabeza, R. (2017). From hippocampus to whole-brain: The role of integrative processing in episodic memory retrieval. *Human Brain Mapping*, *38*(4), 2242–2259. https://doi.org/10.1002/hbm.23518

Gilmore, A. W., Nelson, S. M., & McDermott, K. B. (2016). The Contextual Association Network Activates More for Remembered than for Imagined Events. *Cerebral Cortex*, *26*(2), 611–617. https://doi.org/10.1093/cercor/bhu223

Golland, Y., Golland, P., Bentin, S., & Malach, R. (2008). Data-driven clustering reveals a fundamental subdivision of the human cortex into two global systems. *Neuropsychologia*, *46*(2), 540–553. https://doi.org/10.1016/j.neuropsychologia.2007.10.003

Gonzalez-Castillo, J., Hoy, C. W., Handwerker, D. A., Robinson, M. E., Buchanan, L. C., Saad, Z. S., & Bandettini, P. A. (2015). Tracking ongoing cognition in individuals using brief, whole-brain functional connectivity patterns. *Proceedings of the National Academy of Sciences*, *112*(28), 8762–8767. https://doi.org/10.1073/pnas.1501242112

Gordon, E. M., Laumann, T. O., Adeyemo, B., Huckins, J. F., Kelley, W. M., & Petersen, S. E. (2016). Generation and Evaluation of a Cortical Area Parcellation from Resting-State Correlations. *Cerebral Cortex (New York, N.Y.: 1991)*, *26*(1), 288–303. https://doi.org/10.1093/cercor/bhu239

Gorgolewski, K., Burns, C. D., Madison, C., Clark, D., Halchenko, Y. O., Waskom, M. L., & Ghosh, S. S. (2011). Nipype: A Flexible, Lightweight and Extensible Neuroimaging Data Processing Framework in Python. *Frontiers in Neuroinformatics*, *5*. https://doi.org/10.3389/fninf.2011.00013

Hanley, J. A., & McNeil, B. J. (1982). The meaning and use of the area under a receiver operating characteristic (ROC) curve. *Radiology*, *143*(1), 29–36. https://doi.org/10.1148/radiology.143.1.7063747

Haxby, James. V. (2012). Multivariate pattern analysis of fMRI: The early beginnings. *Neuroimage*, *62*(2), 852–855. https://doi.org/10.1016/j.neuroimage.2012.03.016

Honey, C. J., Newman, E. L., & Schapiro, A. C. (2017). Switching between internal and external modes: A multiscale learning principle. *Network Neuroscience*, *1*(4), 339–356. https://doi.org/10.1162/NETN_a_00024

James, G., Witten, D., Hastie, T., & Tibshirani, R. (2013). *An Introduction to Statistical Learning* (Vol. 103). Springer New York. https://doi.org/10.1007/978-1-4614-7138-7

Ji, J. L., Spronk, M., Kulkarni, K., Repovš, G., Anticevic, A., & Cole, M. W. (2019). Mapping the human brain's cortical-subcortical functional network organization. *NeuroImage*, *185*, 35–57. https://doi.org/10.1016/j.neuroimage.2018.10.006

Kim, D.-Y., Yoo, S.-S., Tegethoff, M., Meinlschmidt, G., & Lee, J.-H. (2015). The inclusion of functional connectivity information into fMRI-based neurofeedback improves its efficacy in the reduction of cigarette cravings. *Journal of Cognitive Neuroscience*, *27*(8), 1552–1572. https://doi.org/10.1162/jocn_a_00802

Kim, H., Daselaar, S. M., & Cabeza, R. (2010). Overlapping brain activity between episodic memory encoding and retrieval: Roles of the task-positive and task-negative networks. *NeuroImage*, *49*(1), 1045–1054. https://doi.org/10.1016/j.neuroimage.2009.07.058

King, D. R., Chastelaine, M. de, Elward, R. L., Wang, T. H., & Rugg, M. D. (2015). Recollection-Related Increases in Functional Connectivity Predict Individual Differences in Memory Accuracy. *Journal of Neuroscience*, *35*(4), 1763–1772. https://doi.org/10.1523/JNEUROSCI.3219-14.2015

Konkle, T., Brady, T. F., Alvarez, G. A., & Oliva, A. (2010). Scene Memory Is More Detailed Than You Think: The Role of Categories in Visual Long-Term Memory. *Psychological Science*, *21*(11), 1551–1556. https://doi.org/10.1177/0956797610385359

Krienen, F. M., Yeo, B. T. T., & Buckner, R. L. (2014). Reconfigurable task-dependent functional coupling modes cluster around a core functional architecture. *Philosophical Transactions of the Royal Society of London. Series B, Biological Sciences*, *369*(1653), 20130526. https://doi.org/10.1098/rstb.2013.0526

Kuhl, B. A., & Chun, M. M. (2014). Successful Remembering Elicits Event-Specific Activity Patterns in Lateral Parietal Cortex. *Journal of Neuroscience*, *34*(23), 8051–8060. https://doi.org/10.1523/JNEUROSCI.4328-13.2014

Kumar, M., Anderson, M. J., Antony, J. W., Baldassano, C., Brooks, P. P., Cai, M. B., Chen, P.-H. C., Ellis, C. T., Henselman-Petrusek, G., Huberdeau, D., Hutchinson, J. B., Li, Y. P., Lu, Q., Manning, J. R., Mennen, A. C., Nastase, S. A., Richard, H., Schapiro, A. C., Schuck, N. W., … Norman, K. A. (2022). BrainIAK: The Brain Imaging Analysis Kit. *Aperture Neuro*, *2021*(4), 42. https://doi.org/10.52294/31bb5b68-2184-411b-8c00-a1dacb61e1da

Lee, H., & Kuhl, B. A. (2016). Reconstructing Perceived and Retrieved Faces from Activity Patterns in Lateral Parietal Cortex. *Journal of Neuroscience*, *36*(22), 6069–6082. https://doi.org/10.1523/JNEUROSCI.4286-15.2016

Lee, S.-H., Kravitz, D. J., & Baker, C. I. (2019). Differential Representations of Perceived and Retrieved Visual Information in Hippocampus and Cortex. *Cerebral Cortex*, *29*(10), 4452–4461. https://doi.org/10.1093/cercor/bhy325

Lenherr, N., Pawlitzek, R., & Michel, B. (2021). New universal sustainability metrics to assess edge intelligence. *Sustainable Computing: Informatics and Systems*, *31*, 100580. https://doi.org/10.1016/j.suscom.2021.100580

Li, Y. P., Cooper, S. R., & Braver, T. S. (2021). The role of neural load effects in predicting individual differences in working memory function. *NeuroImage*, *245*, 118656. https://doi.org/10.1016/j.neuroimage.2021.118656

Linde-Domingo, J., Treder, M. S., Kerrén, C., & Wimber, M. (2019). Evidence that neural information flow is reversed between object perception and object reconstruction from memory. *Nature Communications*, *10*(1), 179. https://doi.org/10.1038/s41467-018-08080-2

Long, N. M., & Kuhl, B. A. (2021). Cortical Representations of Visual Stimuli Shift Locations with Changes in Memory States. *Current Biology: CB*. https://doi.org/10.1016/j.cub.2021.01.004

Manning, J. R., Zhu, X., Willke, T. L., Ranganath, R., Stachenfeld, K., Hasson, U., Blei, D. M., & Norman, K. A. (2018). A probabilistic approach to discovering dynamic full-brain

functional connectivity patterns. *NeuroImage*, *180*, 243–252. https://doi.org/10.1016/j.neuroimage.2018.01.071

Marek, S., & Dosenbach, N. U. F. (2018). The frontoparietal network: Function, electrophysiology, and importance of individual precision mapping. *Dialogues in Clinical Neuroscience*, *20*(2), 133–140.

Miller, E. K., & Cohen, J. D. (2001). An Integrative Theory of Prefrontal Cortex Function. *Annual Review of Neuroscience*, *24*(1), 167–202. https://doi.org/10.1146/annurev.neuro.24.1.167

Norman, K. A., Polyn, S. M., Detre, G. J., & Haxby, J. V. (2006). Beyond mind-reading: Multi-voxel pattern analysis of fMRI data. *Trends in Cognitive Sciences*, *10*(9), 424–430. https://doi.org/10.1016/j.tics.2006.07.005

Norman-Haignere, S. V., McCarthy, G., Chun, M. M., & Turk-Browne, N. B. (2012). Category-Selective Background Connectivity in Ventral Visual Cortex. *Cerebral Cortex*, *22*(2), 391–402. https://doi.org/10.1093/cercor/bhr118

Oppenheim, A. V., & Lim, J. S. (1981). The importance of phase in signals. *Proceedings of the IEEE*, *69*(5), 529–541. https://doi.org/10.1109/PROC.1981.12022

O'Reilly, R. C., & McClelland, J. L. (1994). Hippocampal conjunctive encoding, storage, and recall: Avoiding a trade-off. *Hippocampus*, *4*(6), 661–682. https://doi.org/10.1002/hipo.450040605

Pantazatos, S. P., Talati, A., Pavlidis, P., & Hirsch, J. (2012). Decoding Unattended Fearful Faces with Whole-Brain Correlations: An Approach to Identify Condition-Dependent Large-

Scale Functional Connectivity. *PLOS Computational Biology*, *8*(3), e1002441. https://doi.org/10.1371/journal.pcbi.1002441

Pedregosa, F., Varoquaux, G., Gramfort, A., Michel, V., Thirion, B., Grisel, O., Blondel, M., Prettenhofer, P., Weiss, R., Dubourg, V., Vanderplas, J., Passos, A., Cournapeau, D., Brucher, M., Perrot, M., & Duchesnay, É. (2011). Scikit-learn: Machine Learning in Python. *Journal of Machine Learning Research*, *12*(85), 2825–2830.

Ranganath, C., & Ritchey, M. (2012). Two cortical systems for memory-guided behaviour. *Nature Reviews Neuroscience*, *13*(10), 713–726. https://doi.org/10.1038/nrn3338

Rissman, J., & Wagner, A. D. (2012). Distributed Representations in Memory: Insights from Functional Brain Imaging. *Annual Review of Psychology*, *63*(1), 101–128. https://doi.org/10.1146/annurev-psych-120710-100344

Ritchey, M., & Cooper, R. A. (2020). Deconstructing the Posterior Medial Episodic Network. *Trends in Cognitive Sciences*, *24*(6), 451–465. https://doi.org/10.1016/j.tics.2020.03.006

Robin, J., Hirshhorn, M., Rosenbaum, R. S., Winocur, G., Moscovitch, M., & Grady, C. L. (2015). Functional connectivity of hippocampal and prefrontal networks during episodic and spatial memory based on real-world environments. *Hippocampus*, *25*(1), 81–93. https://doi.org/10.1002/hipo.22352

Rosenberg, M. D., Finn, E. S., Scheinost, D., Papademetris, X., Shen, X., Constable, R. T., & Chun, M. M. (2016). A neuromarker of sustained attention from whole-brain functional connectivity. *Nature Neuroscience*, *19*(1), 165–171. https://doi.org/10.1038/nn.4179

Rosenberg, M. D., Scheinost, D., Greene, A. S., Avery, E. W., Kwon, Y. H., Finn, E. S., Ramani, R., Qiu, M., Constable, R. T., & Chun, M. M. (2020). Functional connectivity predicts changes

in attention observed across minutes, days, and months. *Proceedings of the National Academy of Sciences*, *117*(7), 3797–3807. https://doi.org/10.1073/pnas.1912226117

Rubinov, M., & Sporns, O. (2011). Weight-conserving characterization of complex functional brain networks. *NeuroImage*, *56*(4), 2068–2079. https://doi.org/10.1016/j.neuroimage.2011.03.069

Rugg, M. D., & Vilberg, K. L. (2013). Brain networks underlying episodic memory retrieval. *Current Opinion in Neurobiology*, *23*(2), 255–260. https://doi.org/10.1016/j.conb.2012.11.005

Schacter, D. L., Norman, K. A., & Koutstaal, W. (1998). The Cognitive Neuroscience of Constructive Memory. *Annual Review of Psychology*, *49*(1), 289–318. https://doi.org/10.1146/annurev.psych.49.1.289

Schaefer, A., Kong, R., Gordon, E. M., Laumann, T. O., Zuo, X.-N., Holmes, A. J., Eickhoff, S. B., & Yeo, B. T. T. (2018). Local-Global Parcellation of the Human Cerebral Cortex from Intrinsic Functional Connectivity MRI. *Cerebral Cortex*, *28*(9), 3095–3114. https://doi.org/10.1093/cercor/bhx179

Schedlbauer, A. M., Copara, M. S., Watrous, A. J., & Ekstrom, A. D. (2014). Multiple interacting brain areas underlie successful spatiotemporal memory retrieval in humans. *Scientific Reports*, *4*(1), 6431. https://doi.org/10.1038/srep06431

Shen, X., Finn, E. S., Scheinost, D., Rosenberg, M. D., Chun, M. M., Papademetris, X., & Constable, R. T. (2017). Using connectome-based predictive modeling to predict individual behavior from brain connectivity. *Nature Protocols*, *12*(3), 506–518. https://doi.org/10.1038/nprot.2016.178

Shinkareva, S. V., Mason, R. A., Malave, V. L., Wang, W., Mitchell, T. M., & Just, M. A. (2008). Using fMRI Brain Activation to Identify Cognitive States Associated with Perception of Tools and Dwellings. *PLoS ONE*, *3*(1), e1394. https://doi.org/10.1371/journal.pone.0001394

Shirer, W. R., Ryali, S., Rykhlevskaia, E., Menon, V., & Greicius, M. D. (2012). Decoding Subject-Driven Cognitive States with Whole-Brain Connectivity Patterns. *Cerebral Cortex*, *22*(1), 158–165. https://doi.org/10.1093/cercor/bhr099

Smith, S. M. (2012). The future of FMRI connectivity. *NeuroImage*, *62*(2), 1257–1266. https://doi.org/10.1016/j.neuroimage.2012.01.022

Song, H., Finn, E. S., & Rosenberg, M. D. (2021). Neural signatures of attentional engagement during narratives and its consequences for event memory. *Proceedings of the National Academy of Sciences*, *118*(33). https://doi.org/10.1073/pnas.2021905118

Song, H., & Rosenberg, M. D. (2021). Predicting attention across time and contexts with functional brain connectivity. *Current Opinion in Behavioral Sciences*, *40*, 33–44. https://doi.org/10.1016/j.cobeha.2020.12.007

St Jacques, P. L., Kragel, P. A., & Rubin, D. C. (2011). Dynamic neural networks supporting memory retrieval. *NeuroImage*, *57*(2), 608–616. https://doi.org/10.1016/j.neuroimage.2011.04.039

Stojanoski, B., & Cusack, R. (2014). Time to wave good-bye to phase scrambling: Creating controlled scrambled images using diffeomorphic transformations. *Journal of Vision*, *14*(12), 6. https://doi.org/10.1167/14.12.6

Summerfield, C., Greene, M., Wager, T., Egner, T., Hirsch, J., & Mangels, J. (2006). Neocortical Connectivity during Episodic Memory Formation. *PLOS Biology*, *4*(5), e128. https://doi.org/10.1371/journal.pbio.0040128

Thomaz, C. E., & Giraldi, G. A. (2010). A new ranking method for principal components analysis and its application to face image analysis. *Image and Vision Computing*, *28*(6), 902–913. https://doi.org/10.1016/j.imavis.2009.11.005

Tulving, E. (2002). Episodic memory: From mind to brain. *Annual Review of Psychology*, *53*, 1–25. https://doi.org/10.1146/annurev.psych.53.100901.135114

Turk-Browne, N. B. (2013). Functional Interactions as Big Data in the Human Brain. *Science*, *342*(6158), 580–584. https://doi.org/10.1126/science.1238409

Turk-Browne, N. B., Norman-Haignere, S. V., & McCarthy, G. (2010). Face-Specific Resting Functional Connectivity between the Fusiform Gyrus and Posterior Superior Temporal Sulcus. *Frontiers in Human Neuroscience*, *4*, 176. https://doi.org/10.3389/fnhum.2010.00176

Vuilleumier, P., & Pourtois, G. (2007). Distributed and interactive brain mechanisms during emotion face perception: Evidence from functional neuroimaging. *Neuropsychologia*, *45*(1), 174–194. https://doi.org/10.1016/j.neuropsychologia.2006.06.003

Wang, Y., Cohen, J. D., Li, K., & Turk-Browne, N. B. (2015). Full correlation matrix analysis (FCMA): An unbiased method for task-related functional connectivity. *Journal of Neuroscience Methods*, *251*, 108–119. https://doi.org/10.1016/j.jneumeth.2015.05.012

Watanabe, T., Kimura, H. M., Hirose, S., Wada, H., Imai, Y., Machida, T., Shirouzu, I., Miyashita, Y., & Konishi, S. (2012). Functional dissociation between anterior and posterior temporal

cortical regions during retrieval of remote memory. *The Journal of Neuroscience: The Official Journal of the Society for Neuroscience*, *32*(28), 9659–9670. https://doi.org/10.1523/JNEUROSCI.5553-11.2012

Westphal, A. J., Wang, S., & Rissman, J. (2017). Episodic Memory Retrieval Benefits from a Less Modular Brain Network Organization. *Journal of Neuroscience*, *37*(13), 3523–3531. https://doi.org/10.1523/JNEUROSCI.2509-16.2017

Woolrich, M. W., Ripley, B. D., Brady, M., & Smith, S. M. (2001). Temporal Autocorrelation in Univariate Linear Modeling of FMRI Data. *NeuroImage*, *14*(6), 1370–1386. https://doi.org/10.1006/nimg.2001.0931

Xiao, X., Dong, Q., Gao, J., Men, W., Poldrack, R. A., & Xue, G. (2017). Transformed Neural Pattern Reinstatement during Episodic Memory Retrieval. *The Journal of Neuroscience*, *37*(11), 2986–2998. https://doi.org/10.1523/JNEUROSCI.2324-16.2017

Yeo, B. T. T., Krienen, F. M., Sepulcre, J., Sabuncu, M. R., Lashkari, D., Hollinshead, M., Roffman, J. L., Smoller, J. W., Zöllei, L., Polimeni, J. R., Fischl, B., Liu, H., & Buckner, R. L. (2011). The organization of the human cerebral cortex estimated by intrinsic functional connectivity. *Journal of Neurophysiology*, *106*(3), 1125–1165. https://doi.org/10.1152/jn.00338.2011

Yeshurun, Y., Nguyen, M., & Hasson, U. (2021). The default mode network: Where the idiosyncratic self meets the shared social world. *Nature Reviews Neuroscience*, 1–12. https://doi.org/10.1038/s41583-020-00420-w